



National Library
of Canada

Bibliothèque nationale
du Canada

Canadian Theses Service

Service des thèses canadiennes

Ottawa, Canada
K1A 0N4

NOTICE

The quality of this microform is heavily dependent upon the quality of the original thesis submitted for microfilming. Every effort has been made to ensure the highest quality of reproduction possible.

If pages are missing, contact the university which granted the degree.

Some pages may have indistinct print especially if the original pages were typed with a poor typewriter ribbon or if the university sent us an inferior photocopy.

Reproduction in full or in part of this microform is governed by the Canadian Copyright Act, R.S.C. 1970, c. C-30, and subsequent amendments.

AVIS

La qualité de cette microforme dépend grandement de la qualité de la thèse soumise au microfilmage. Nous avons fait tout ce qui est en notre pouvoir pour assurer une qualité supérieure de reproduction.

S'il manque des pages, veuillez communiquer avec l'université qui a conféré le grade.

La qualité d'impression de certaines pages peut laisser à désirer, surtout si les pages originales ont été dactylographiées à l'aide d'un ruban usé ou si l'université nous a fait parvenir une photocopie de qualité inférieure.

La reproduction, même partielle, de cette microforme est soumise à la Loi canadienne sur le droit d'auteur, SRC 1970, c. C-30, et ses amendements subséquents.

UNIVERSITY OF ALBERTA

IN VIVO DETERMINATION OF INSULIN SENSITIVITY IN RATS BY MINIMAL
MODEL / FREQUENTLY SAMPLED INTRAVENOUS GLUCOSE TOLERANCE TEST

BY

ZHONG-XIAO CHEN

A THESIS

SUBMITTED TO THE FACULTY OF GRADUATE STUDIES AND
RESEARCH IN PARTIAL FULFILLMENT OF THE REQUIREMENTS FOR
THE DEGREE OF MASTER OF SCIENCE

IN

EXPERIMENTAL MEDICINE

DEPARTMENT OF MEDICINE

EDMONTON, ALBERTA

(SPRING) (1991)



National Library
of Canada

Bibliothèque nationale
du Canada

Canadian Theses Service Service des thèses canadiennes

Ottawa, Canada
K1A 0N4

The author has granted an irrevocable non-exclusive licence allowing the National Library of Canada to reproduce, loan, distribute or sell copies of his/her thesis by any means and in any form or format, making this thesis available to interested persons.

The author retains ownership of the copyright in his/her thesis. Neither the thesis nor substantial extracts from it may be printed or otherwise reproduced without his/her permission.

L'auteur a accordé une licence irrévocable et non exclusive permettant à la Bibliothèque nationale du Canada de reproduire, prêter, distribuer ou vendre des copies de sa thèse de quelque manière et sous quelque forme que ce soit pour mettre des exemplaires de cette thèse à la disposition des personnes intéressées.

L'auteur conserve la propriété du droit d'auteur qui protège sa thèse. Ni la thèse ni des extraits substantiels de celle-ci ne doivent être imprimés ou autrement reproduits sans son autorisation.

ISBN 0-215-66614-5

Canada

UNIVERSITY OF ALBERTA

RELEASE FORM

NAME OF AUTHOR: ZHONG-XIAO CHEN

TITLE OF THESIS: *IN VIVO* DETERMINATION OF INSULIN SENSITIVITY
IN RATS BY MINIMAL MODEL / FREQUENTLY SAMPLED
INTRAVENOUS GLUCOSE TOLERANCE TEST

DEGREE: MASTER OF SCIENCE

YEAR THIS DEGREE GRANTED: 1991

PERMISSION IS HEREBY GRANTED TO THE UNIVERSITY OF ALBERTA
LIBRARY TO REPRODUCE SINGLE COPIES OF THIS THESIS AND TO LEND OR
SELL SUCH COPIES FOR PRIVATE, SCHOLARLY OR SCIENTIFIC RESEARCH
PURPOSE ONLY.

THE AUTHOR RESERVES OTHER PUBLICATION RIGHTS, AND NEITHER THE
THESIS NOR EXTENSIVE EXTRACTS FROM IT MAY BE PRINTED OR OTHERWISE
REPRODUCED WITHOUT THE AUTHOR'S WRITTEN PERMISSION.

Zhong-xiao Chen
(Student's Signature)

#8, 10625-85 Ave.

(Student's Permanent Address)

Edmonton, Alberta. T6E 2K6

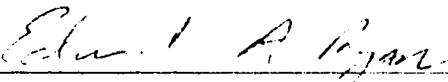
Date: April 24, 91

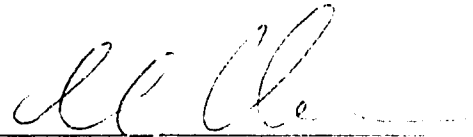
UNIVERSITY OF ALBERTA

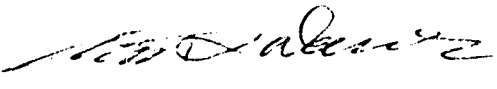
FACULTY OF GRADUATE STUDIES AND RESEARCH

THE UNDERSIGNED CERTIFY THAT THEY HAVE READ, AND
RECOMMENDED TO THE FACULTY OF GRADUATE STUDIES AND
RESEARCH FOR ACCEPTANCE, A THESIS
ENTITLED IN VIVO DETERMINATION OF INSULIN SENSITIVITY IN RATS BY
MINIMAL MODEL / FREQUENTLY SAMPLED INTRAVENOUS GLUCOSE TOLERANCE
TEST
SUBMITTED BY ZHONG-XIAO CHEN
IN PARTIAL FULFILLMENT OF THE REQUIREMENTS FOR THE
DEGREE OF MASTER OF SCIENCE IN EXPERIMENTAL MEDICINE.


DR. DIANE T. FINEGOOD


DR. EDMOND A. RYAN


DR. CHRIS I. CHEESEMAN


DR. GARTH L. WARNOCK

Date: April 19, 1991

ABSTRACT

The minimal model method has been developed and validated in large animals and humans to estimate *in vivo* insulin action and glucose metabolism. The present studies were carried out to determine if the model could be applied to the rat, by modification of the frequently sampled intravenous glucose tolerance test (FSIGT) protocol, to achieve reliable and accurate estimation of the parameters. Glucose (300 mg/kg) was injected at 0 minute and frequent blood samples were taken for glucose and insulin concentrations. Insulin sensitivity (S_I) and glucose effectiveness (S_G) could be estimated from the GLUCOSE protocol with only 7 or 8 blood samples, but the fractional standard deviation (FSD) and the identifiability were poor. The protocol was modified by additional injections of somatostatin just prior to glucose and tolbutamide at 8 minutes. Experimental results suggested that the parameter estimation was significantly improved by the modified protocol as compared to the GLUCOSE protocol. Computer simulation was applied to test four protocols: {GLUCOSE} (GLU), {SOMATOSTATIN + GLUCOSE} (SRF), {GLUCOSE + TOLBUTAMIDE} (TOL), and {SOMATOSTATIN + GLUCOSE + TOLBUTAMIDE} (SGT). The SRF and SGT protocols resulted in overall better quantification of parameters evidenced by simulation. The number of samples, in particular for glucose, were increased without further blood loss, such that the dynamic changes of glucose and insulin could be better characterized. The identifiability was 100 % and FSD was plausible with a protocol of 24 blood samples. A {GLUCOSE + INSULIN} protocol was performed in control and high-fat-diet fed animals, the results indicated that without somatostatin injection, the model may not

be able to differentiate the parameters S_I and S_G . In conclusion: 1) The parameters of the minimal model can be obtained from the rat FSIGT experiments with only 7 or 8 samples; 2) With the increased number of blood samples, the ability of the model to quantify the parameters can be markedly improved; and 3) Somatostatin must be added in the rat FSIGT experiment to augment the model's ability to differentiate the parameters S_I and S_G .

ACKNOWLEDGEMENTS

I would like to express my greatest gratitude to my supervisors Dr. Diane Finegood and Dr. Edmond Ryan. Their guidance, patience, and encouragement made it possible for me to persevere through the years of study. Their help and support throughout the study are gratefully acknowledged. I am deeply indebted to them.

I would like to thank the members of my supervisory committee, Dr. Chris Cheeseman, and Dr. Garth Warnock, for their valuable guidance and suggestions to the study. I would also like to thank Dr. William McBlain for his suggestions and help during my study. Without their help this thesis would not have been completed as easily.

I would express my grateful appreciation to Dr. Susan Jacobos and her technical staff for their assistance. Also I would like to thank Mr. Todd Lang, Ms. JiPing Tang, and Ms. Amy Schwartz for their assistance with this work.

I would especially thank my husband, Bing-Yan Zhu for his support and help.

TABLE OF CONTENTS

CHAPTER I INTRODUCTION	
1. GLUCOSE REGULATION AND INSULIN ACTION.....	1
GLUCOSE HOMEOSTASIS AND ITS REGULATION.....	1
INSULIN SECRETION AND ACTION.....	3
2. INSULIN RESISTANCE AND GLUCOSE INTOLERANCE.....	6
3. METHODOLOGIES OF <i>IN VIVO</i> ESTIMATION OF INSULIN SENSITIVITY...9	
INSULIN-GLUCOSE TEST.....	9
GLUCOSE TOLERANCE TEST.....	10
PANCREATIC SUPPRESSION TEST.....	11
GLUCOSE CLAMP TECHNIQUE.....	15
MINIMAL MODEL/FSIGT TECHNIQUE.....	26
4. HIGH FAT DIET AND INSULIN RESISTANCE.....	35
5. RATIONALE.....	35
6. RESEARCH OBJECTIVES.....	38
CHAPTER II METHODS	
SUMMARY.....	40
SURGICAL PREPARATION.....	40
FSIGT EXPERIMENT.....	44
DATA ANALYSIS.....	45
CHAPTER III RESULTS	
OVERVIEW OF STUDIES.....	46
GROUP 1. GLUCOSE PROTOCOL IN LONG EVANS RAT.....	47
GROUP 2. GLUCOSE COMBINED WITH SRIF AND TOLB PROTOCOL IN LONG EVANS RAT.....	56
GROUP 3. FSIGT EXPERIMENT IN SPRAGUE-DAWLEY RAT.....	63
GROUP 4. SIMULATION.....	69
GROUP 5. INSULIN DOSE RESPONSE / HIGH FAT DIET STUDY.....	78
CHAPTER IV DISCUSSION	
1. SUMMARY.....	96
2. ADAPTATION OF MINIMAL MODEL/FSIGT TO RAT.....	97

3. THE NUMBER OF BLOOD SAMPLES.....	99
4. HIGH FAT DIET.....	102
5. INSULIN DOSE RESPONSE STUDY.....	103
6. COMPUTER SIMULATION.....	104
7. THE ROLE OF SOMATOSTATIN IN RAT FSIGT.....	105
8. CONCLUSIONS.....	109
REFERENCES.....	110

LIST OF TABLES

TABLE 1. The effect of high fat diet on <i>in vivo</i> insulin action.....	36
TABLE 2. The effect of high fat diet on <i>in vitro</i> insulin action.....	37
TABLE 3. Data of {GLUCOSE} protocol in Long Evans rat FSIGT.....	53
TABLE 4. Parameters of {GLUCOSE} protocol in LE rat FSIGT.....	57
TABLE 5. Comparison of {GLUCOSE} and modified protocols in LE rat FSIGT.....	62
TABLE 6. Computer simulation.....	75
TABLE 7. The summary of computer simulation.....	77
TABLE 8. Components of standard chow diet and high fat diet.....	79
TABLE 9. Rat FSIGT in insulin dose response / high fat diet study.....	91
TABLE 10. Summary of FSIGT in insulin dose response / high fat diet study.....	94

LIST OF FIGURES

FIGURE 1. Minimal model of glucose disappearance.....	27
FIGURE 2. The mean time course of glucose and insulin dynamics in LE rat: GLUCOSE protocol.....	48
FIGURE 3. The glucose and insulin dynamics of individual GLUCOSE protocols in LE rat.....	51
FIGURE 4. An example of rat FSIGT: GLUCOSE protocol.....	54
FIGURE 5. The mean glucose and insulin kinetics of SGT protocols.....	59
FIGURE 6. The glucose and insulin dynamics in SD rat: GLU and SGT protocols.....	65
FIGURE 7. The parameters of FSIGT in SD rat: comparison of the GLU and SGT protocols.....	67
FIGURE 8. Schematic of the simulation process.....	70
FIGURE 9. The four insulin profiles in simulation.....	73
FIGURE 10. An experiment of {GLUCOSE + INSULIN} protocol.....	82
FIGURE 11. A section of insulin dynamics in the {GLUCOSE + INSULIN} FSIGT.....	84
FIGURE 12. The insulin areas vs. the insulin doses in the insulin dose response study.....	86
FIGURE 13. The glucose disappearance rate in the insulin dose response study.....	89

INTRODUCTION

1. Glucose Regulation and Insulin Action

(1). Glucose homeostasis and its regulation

Carbohydrate is a primary source of fuel for the whole body. All cells can use glucose for energy and some cells virtually consume only glucose, such as mature erythrocytes [1]. The blood glucose concentration is maintained in a relatively constant range despite the intermittent feeding behavior of man. The blood glucose level is determined by the net balance between glucose utilization (disappearance from the blood) and glucose production (entry into the blood). This glucose homeostasis results from multiple regulatory mechanisms involving many factors. Insulin is considered to be the primary regulator.

Glucose uptake and utilization by muscle, fat and liver are controlled by insulin. The central nervous system, erythrocytes and the renal medulla constitute the major tissues in which glucose metabolism is not regulated by insulin [2]. The overall effect of insulin is anticatabolic with anabolic regulation of carbohydrate, protein and lipid metabolism. The net results of insulin action are manifested as a decrement in blood glucose, amino acids and free fatty acids [2].

In the fasting state, the major site of glucose uptake is the brain, smaller amounts of glucose being utilized by the blood cells and by

resting muscle [2]. Approximately 75% or more of glucose utilization during fasting is not dependent on insulin [2]. This glucose is disposed of by tissues not dependent on insulin, e.g., brain, gastrointestinal tract, erythrocytes, renal medulla, as well as by the insulin sensitive tissues where glucose uptake is dependent only on glucose itself at basal insulin levels, without the effect of elevated insulin [3]. During the postabsorptive state an important effect of the basal plasma insulin on glucose homeostasis is the promotion of glucose production such that normoglycemia is maintained [2]. If insulin levels fall below normal fasting concentrations, e.g., insulin deficiency in untreated ketoacidosis, hepatic glucose production increases markedly [4] and results in fasting hyperglycemia.

Food ingestion elevates the blood glucose level via intestinal glucose absorption. Normal blood glucose levels are restored by increasing glucose uptake via facilitated diffusion and by suppressing hepatic glucose output (HGO) via a negative feed-back mechanism. The increase in the plasma glucose also stimulates insulin secretion. Elevated insulin increases glucose uptake by insulin sensitive tissues and suppresses HGO [6]. Thus, insulin sensitivity can be considered to be the ability of incremental insulin concentrations to augment glucose disappearance from plasma.

Because glucose transport across the plasma membrane is mediated by a transport protein, the effect of insulin on glucose uptake is dependent on the ambient glucose concentration [7, 8], and insulin's action to activate and translocate carrier protein to the cell membrane.

Therefore, insulin action can be considered to synergize the ability of glucose to normalize its own concentration. During the fed state, approximately 75% of the total glucose ingested is utilized via the insulin-mediated glucose uptake into insulin sensitive tissues [9].

(2). Insulin secretion and action

Insulin is a polypeptide hormone secreted by β cells of the pancreatic islets of Langerhans. Preproinsulin is synthesized in ribosomes attached to the rough endoplasmic reticulum (RER) in the β cells. Preproinsulin is cleaved in the RER yielding proinsulin, which is transferred to the Golgi apparatus by transitional budding from RER. Proinsulin-containing granules are condensed and bud from the Golgi, migrate towards the plasma membrane, and transform into mature secretory granules in which proinsulin is cleaved into insulin and connecting-peptide (C-peptide). The secretory vesicles marginate and fuse with the plasma membrane and release their content into the extracellular space by exocytosis. Insulin then crosses the capillary endothelial barrier to reach the blood circulation [10]. This insulin synthesis and secretion sequence is regulated by a variety of parameters including nutritional, hormonal, and neurophysiological factors [11]. Glucose serves as a prominent secretagogue by exerting its stimulatory effects on the biosynthesis of insulin [12] and on the margination and exocytosis of insulin secretory granules [13].

Insulin is delivered by the circulation to the peripheral capillaries, and transported across the capillary endothelium layer into

the interstitium via a receptor-mediated process [107, 109], where insulin binds to its receptor on the target cell. The cellular effects of insulin are diverse [15]. Insulin modulates many cellular events, including the transportation of molecules across the plasma membrane; activities of key enzymes in intermediary metabolism; rates of protein synthesis and degradation; rates of DNA and RNA synthesis; and cellular growth and differentiation.

The binding of insulin to its receptor is the initial step of insulin action. The insulin receptor is a tetramer composed of two α -subunits and two β -subunits linked by disulfide bonds. The extracellular α -subunits have insulin binding domains and the β -subunits transverse the plasma membrane and have protein tyrosine kinase in the cytosolic segments. The mechanisms of signal transduction for insulin are not completely known; however, hypotheses have been proposed with experimental support. The binding of insulin to the α -subunits stimulates autophosphorylation of tyrosine residues on the intracellular domains of the β -subunits [16, 19]. The autophosphorylation of the insulin receptor triggers the activation of a ligand-independent tyrosine kinase which presumably leads to a cascade of phosphorylations of substrates [19, 26]. The protein tyrosine kinase is essential for many of insulin's actions. Saltiel proposed that two distinct pathways of signal transduction coordinate intracellular changes in protein phosphorylation: a phosphorylation cascade initiated by the tyrosine kinase activity of the receptor, and the generation of a second messenger [15]. The two pathways may operate synergistically to produce the series of cellular responses to insulin. The proposed second

messenger has a structure of an inositol glycan and acts in a manner analogous to cyclic nucleotides or inositol phosphates. By activation of protein phosphatases and protein kinases, the activities of some enzymes can be regulated by dephosphorylation and phosphorylation, e.g., glycogen synthetase, pyruvate dehydrogenase, acetyl-CoA carboxylase, and ATP-citrate lyase, which catalyze different pathways of fuel metabolism.

In the insulin sensitive tissues (fat and muscle), insulin stimulates the glucose uptake which occurs by facilitated diffusion via glucose transporters (GLUT) in the plasma membrane. In fact, all cells express glucose transporters, and families of transporters have been characterized and their amino acid sequences have been deduced [14, 17]. Five glucose transporters have been identified, named GLUT1 to GLUT5. The insulin sensitive glucose transporter, GLUT4 (muscle/fat), has been found in both the plasma membrane and an intracellular pool (low-density microsomes). Following binding of insulin to its receptor, the intracellular GLUT4 was activated, mobilized and inserted into the plasma membrane so that the number of transporters in the membrane, as well as, their intrinsic activities were increased [14]. The GLUT4 recycled to their intracellular pool when insulin was withdrawn. In human skeletal muscle, acute insulin treatment caused recruitment of glucose transporters to the plasma membrane, and prolonged exposure to insulin could increase expression of GLUT1 mRNA and GLUT1 protein [18], which was distributed in most cells responsible for constitutive glucose uptake. The mechanism by which insulin stimulates translocation of glucose transporters remains to be clarified. The transduction may be

mediated by a phosphorylation cascade or may involve the guanine nucleotide-binding protein G_s and protein kinase C [49].

Following the insulin-receptor interaction, the ligand-receptor complexes move along the plasma membrane to the coated pits, and concentrate in these membrane invaginations, where the insulin-receptor complexes are internalized through endocytosis [19]. This process results in the formation of coated vesicles in the cytoplasm. The coated vesicles lose their coats, which are made of the protein clathrin, by as yet unknown mechanisms. The complexes are then found in endosomes which are endowed with proton pumps capable of acidifying their internal milieu. The ligands are dissociated from the receptors in the acidic environment [19]. The insulin reaches the digestive vacuoles, i.e., secondary lysosomes, where insulin is degraded. Alternatively the receptors are recycled to the plasma membrane before reaching the lysosomes. The internalization of the ligand-receptor complex and the degradation of insulin are crucial to the desensitization and termination of the hormonal signal.

2. Insulin Resistance and Glucose Intolerance

Diabetes was thought to be entirely due to insulin deficiency before the late 1930's. At that time Himsworth suggested and it was afterwards confirmed by the radioimmunoassay of the plasma insulin level, that diabetes mellitus could be divided into insulin-sensitive and non-insulin sensitive types. Indeed, insulin resistance exists in many patho- and physiological situations, such as obesity [27, 28, 29],

pregnancy [71], high fat diet [20, 21], aging [72], chronic uremia [67], liver cirrhosis [76, 77], trauma [22, 23], hypertension [24], and type I [73, 74] and type II diabetes [79].

Glucose tolerance is determined by a complex system involving glucose sensing, insulin secretion, transportation of insulin molecules, the actions of insulin, and the ability of glucose per se to normalize its own concentration. Defects in any of these factors may lead to glucose intolerance. These defects can be classified into three categories [25]. (I) Insufficient or abnormal β cell secretory products. Either a mutation in the insulin gene can lead to a biologically defective insulin molecule or the conversion of proinsulin to insulin is incomplete. (II) Circulating insulin antagonists. Elevated plasma hormonal and non-hormonal insulin antagonists include glucocorticoids (Cushing's syndrome), growth hormone (acromegaly), placental lactogen (pregnancy), glucagon, catecholamines, and free fatty acids. The existences of anti-insulin and anti-insulin receptor antibodies can also cause insulin resistance. (III) Target tissue defects in insulin action. Reduction in the numbers of cellular insulin receptors and in receptor intrinsic activity or affinity can be considered as receptor defects. The post-receptor defects might include abnormalities in the coupling mechanism between the insulin-receptor complex and the glucose transport system, in the glucose transport system, or in the intracellular enzyme activity of the various pathways of glucose metabolism.

Numerous publications have demonstrated that insulin resistance is a prominent characteristic of obesity and non-insulin dependent diabetes mellitus (NIDDM). In obesity, insulin resistance appears to be heterogeneous and due to combined receptor binding and postreceptor binding defects at the target tissue level [27, 28]. Mild insulin resistance displays only the receptor defect due to both reduced receptor numbers [27] and abnormal coupling between binding and postbinding events [29], whereas more severe insulin resistance is typically characterized by a postreceptor defect [25] manifested as reduced maximal insulin responsiveness. The magnitude of this postreceptor defect is positively related to the degree of hyperinsulinemia [27].

Although both impaired insulin secretion and insulin resistance contribute to the pathogenesis of type II diabetes, insulin resistance appears to be present in all NIDDM patients. Since the majority of NIDDM patients are overweight (approximately 80%), obesity is closely related to NIDDM. However, insulin resistance exists in NIDDM independent of obesity. Obese NIDDM subjects exhibit greater insulin resistance than non-diabetic obese subjects [31] and lean NIDDM patients are also insulin resistant [32]. Combined binding and postbinding defects, i.e., insulin receptor defects, abnormal signal transduction, and impaired glucose transport system (both reduced numbers and intrinsic activity of glucose transporters), may be responsible for insulin resistance in NIDDM [30].

3. Methodologies of *In Vivo* Estimation of Insulin Sensitivity

Many of the investigations of insulin action have been carried out *in vitro* to help our understanding of the occurrences and mechanisms of insulin insensitivity; e.g., studies on insulin-receptor binding (calculation of the affinity and the number of receptors), glucose transport system, glucose uptake, and glucose metabolism by oxidative and non-oxidative pathways. However, it is also important and critical to quantify insulin sensitivity and define insulin resistance *in vivo* at the whole body level. Several techniques which have been previously employed to measure insulin sensitivity are briefly discussed.

(1). Insulin-Glucose test

In the 1930's, Himsworth introduced the insulin-glucose tolerance test to measure insulin sensitivity *in vivo* in diabetic subjects [33,34,35]. An individual received two oral glucose tolerance tests; one of which had an intravenous (i.v.) insulin injection prior to the oral glucose load (insulin-glucose test). The areas under the blood sugar curves were determined; and the difference between the area of the glucose tolerance curve and the area of the insulin-glucose tolerance curve could be viewed as the measurement of the effect of the injected insulin. Himsworth defined insulin sensitivity as the ratio of the glucose area from the insulin-glucose test to that of glucose tolerance test. He demonstrated insulin insensitivity in aging [36] and in obese non-diabetic subjects [35].

Himsworth's method was inferential as various mechanisms could influence the measurement of insulin sensitivity. These factors include differences in gastrointestinal glucose absorption, endogenous insulin release in response to glucose, variation in the inhibitory effects of injected insulin on endogenous insulin secretion, and differences in rates of insulin clearance. Following the development of the insulin radioimmunoassay by Yalow and Berson in 1960 [37], other methods were developed for *in vivo* quantification of insulin sensitivity.

(2). Glucose tolerance test (GTT)

Oral (OGTT) and intravenous glucose tolerance tests (IVGTT), during which both glucose and insulin concentrations were intermittently measured for 3 hrs after a glucose load, was employed for the determination of insulin sensitivity *in vivo*. Insulin insensitivity is evident as hyperinsulinemia at the face of a normal or supranormal plasma glucose patterns during glucose tolerance testing [38,39]. Diminished insulin sensitivity has been demonstrated in obese non-diabetics [40], patients with diabetes mellitus [41], aging [42,43], pregnancy and patients with gestational diabetics [44,45] by means of the glucose tolerance test.

There is, however, a continuous interaction between the β cells of the pancreatic islets and the insulin-target tissues during a GTT. That is, changes in the plasma glucose level stimulate insulin secretion from the β cells; and the released insulin will affect the plasma glucose concentration. This closed-loop relationship between glucose and

insulin limits the interpretation of the results of glucose tolerance testing such that the relative contributions to glucose tolerance of β cell function and insulin sensitivity cannot be distinctly quantified.

The difficulty of interpreting closed loop data was illustrated by computer simulation [46]. The simulation predicted that an 86% decrease in insulin sensitivity without other defects would not result in impaired glucose tolerance because hyperglycemia caused by insulin insensitivity can be compensated for by the β cell response. Likewise, in the insulin insensitive individual with up to 75% decrement in β cell function, the integrated insulin response would not be less than in a normal subject. As a result of the difficulties in interpreting closed loop data, it is necessary to utilize an approach which opens the glucose-insulin feedback loop. Two techniques have been widely applied in animals and humans to quantify insulin sensitivity *in vivo*: the pancreatic suppression test and the glucose clamp.

(3). Pancreatic suppression test (PST)

A. Principle

Reaven et al. introduced the pancreatic or insulin suppression test (PST or IST) in 1970 [47], in which pharmacological agents were used to block pancreatic insulin release in response to an elevated plasma glucose concentration. Commonly epinephrine and propranolol infusion (E/P) or alternatively somatostatin (SRIF) infusion were employed to inhibit the endogenous insulin secretion. Simultaneously exogenous

glucose and insulin were infused at a constant rate at which plasma insulin was raised to a physiological concentration (approximately 100 $\mu\text{U/ml}$). After a period of equilibration (usually 90 min), plasma insulin and glucose levels reached a steady-state. Thus, the levels of steady-state plasma glucose (SSPG, defined as the average glucose during the steady-state observation period) at fixed rates of insulin and glucose infusion represented the measurement of tissue sensitivity to insulin.

A fundamental assumption of the PST was that the combined infusions of epinephrine, propranolol, glucose and insulin would absolutely inhibit endogenous glucose production [47, 48]. Under this condition, the exogenous glucose infusion (GINF) was the total entry of glucose into the body. When steady-state plasma glucose and insulin levels were achieved, GINF (glucose appearance) should equal the total glucose utilization (glucose disappearance) which was composed of insulin-independent and insulin-dependent glucose uptake. Therefore, for a given rate of glucose infusion, SSPG would represent the efficiency of both glucose-mediated and insulin-mediated glucose clearance.

In the normal individual, SSPG is near the basal level. In the case of insulin resistance, the insulin-dependent glucose utilization is reduced. This reduction of glucose outflow from the plasma into the insulin sensitive tissues will force the plasma glucose to rise and reach a higher steady-state level, at which the greater impetus increases the peripheral glucose uptake via both mass action and insulin-stimulated effect. Thus, the new balance between glucose influx

and efflux is achieved at a higher SSPG in the insulin-insensitive state.

B. Application

The PST has been applied to estimate insulin sensitivity in both human and experimental animals. Insulin resistance was demonstrated in subjects with various states of glucose intolerance and diminished insulin sensitivity, including NIDDM [50, 51], impaired glucose tolerance [52], obesity [53, 54], as well as, insulin-dependent diabetes mellitus (IDDM) and ketoacidosis [55, 56]. Dogs made diabetic with alloxan treatment had a significantly higher SSPG [57]. Insulin insensitivity was reported in streptozotocin-induced diabetic rats [58] in which exercise could reverse the insulin sensitivity to normal. The insulin resistance was also found in aging rats using the PST [59].

In order to compare SSPG among individuals, it is ideal to match steady-state plasma insulin (SSPI) levels in different individuals by adjusting the rate of insulin infusion. Nevertheless, identical SSPI may not be true in many situations, and the relationship between SSPG and SSPI is nonlinear in man [60] and rats [59]. Thus, increased SSPG may not reflect the proportional decline in insulin sensitivity, and the comparison of insulin sensitivity (SSPG/SSPI) among individuals with different SSPI levels would not necessarily be accurate.

C. Interpretation of SSPG

Although the SSPG largely reflects the degree of insulin sensitivity, glucose-mediated glucose utilization cannot be derived directly from the PST. Approximately 75% of basal glucose clearance was estimated as glucose's effect on its own clearance [2]. However, SSPG may vary from the basal plasma glucose level and among individuals. Therefore, the glucose-dependent glucose clearance at steady-state would be different from basal as well as among individuals since various levels of SSPG could result in a different impetus for glucose uptake via facilitated diffusion. SSPG is determined by the effect of both glucose and insulin, thus the inconsistency of glucose effect at various SSPG levels could influence the estimation of insulin sensitivity.

Though the pancreatic suppression test was the first direct measure of insulin sensitivity, many factors may influence the quantification of insulin action. The effects of combined infusion, the stability of SSPG, and the various degrees in suppression of hepatic glucose production among individuals could affect the measurement of insulin sensitivity. The inability of the PST to determine the difference between the non-insulin-mediated and insulin-mediated glucose utilization could further contribute to the error in the estimation of insulin sensitivity.

(4). Glucose Clamp Technique

A. Principle

As discussed, the existences of the glucose-insulin feedback inter-relationship complicates the estimation of insulin action. Another technique, the glucose clamp, which was developed and introduced by Andres and his colleagues [61-64], interrupts the feedback loop by externally controlling the blood glucose and insulin concentrations. During the clamp studies, the plasma glucose is maintained constant by a exogenous insulin and glucose infusion. In contrast to the PST, the maintenance of basal blood glucose during the clamp eliminates the counter-regulatory response which may confound the glucose regulation and influence the estimation of insulin sensitivity during the PST in an insulin-sensitive individual. No pharmacological agents are required for the inhibition of glucose production in the clamp in comparison with the PST. Over the last 15 years, the glucose clamp method has been widely employed by many groups of investigators for the *in vivo* determination of insulin sensitivity in human subjects and experimental animals.

Insulin sensitivity determination is usually accomplished by using a euglycemic clamp and the quantification of β cell sensitivity to glucose can be determined by hyperglycemic clamping.

Euglycemic clamp: Fasting plasma glucose is relatively constant for a given individual, thus glucose production (R_a) should be equal to

glucose utilization (R_d) in the postabsorptive state. In the euglycemic clamp, exogenous insulin is infused at a predetermined rate to raise the plasma insulin to a desired level (commonly $100 \mu\text{U}/\text{ml}$, [64]). Insulin infusion lowers the plasma glucose by increasing R_d and decreasing R_a . This decline of blood glucose is compensated by a rate of exogenous glucose infusion which is calculated to match the effect of insulin on lowering plasma glucose. Arterial blood is frequently sampled to determine glucose values and to adjust the rate of glucose infusion in order to maintain the basal glucose level. After a period of equilibration, plasma insulin and glucose reach a steady-state, and the glucose infused to maintain euglycemia (M) is considered to indicate the insulin action at the prevailing insulin level (I). The ratio of glucose infusion (corrected for urine loss) to the plasma insulin (M/I) is the measure of the quantity of glucose metabolized per unit of plasma insulin concentration and thus is the index of insulin sensitivity [64, 67]. The underlying assumptions of this calculation are that the endogenous glucose production is completely suppressed, and that the M is linearly related to I , and there is no intercept of M on I .

Hyperglycemic clamp: In the postabsorptive state, plasma glucose is acutely elevated by exogenous glucose infusion. After the desired hyperglycemia is achieved, the hyperglycemic plateau is maintained by adjustment of the glucose infusion rate. When the steady-state glycemia plateau is held, the glucose infusion rate is essentially a measure of glucose tolerance (index of glucose metabolism), and the plasma insulin response to the fixed hyperglycemia is a measure of β cell response to glucose [64, 67]. DeFronzo et al. [64] also reported that the insulin

response to the sustained hyperglycemia was biphasic, with an early burst of insulin release (0-10 min) followed by a phase of gradually increasing insulin concentration until the end of the study (10-120 min). The quantification of two phases of insulin secretion is particularly important because it has been suggested that the loss of the initial phase of insulin response is the earliest detectable abnormality in diabetes [65, 66].

When the glucose clamp technique is used in conjunction with isotopic measurement of glucose turnover, the individual effect of insulin on glucose production and glucose utilization can be estimated [67, 27]. A primed continuous infusion of [$3\text{-}^3\text{H}$]glucose is frequently used. Endogenous glucose production (R_a) and glucose utilization (alternatively, glucose disappearance, glucose uptake, or glucose disposal; R_d) are calculated from the glucose specific activity during the steady-state plateau using the tracer dilution method of Steele et al. [68].

B. Insulin dose-response curve

A fixed rate of insulin infusion may result in different levels of steady-state insulin in various individuals as the metabolic clearance rate of insulin may not be the same. It is difficult to obtain a desired steady-state insulin concentration from a predetermined rate of insulin infusion and to match insulin levels between individuals. Therefore, the comparison of insulin sensitivity may not be appropriate

since the insulin levels could be different between individual experiments.

The insulin dose-response curve for glucose metabolism can better characterize the action of insulin. Alteration of insulin action may be due to changes in insulin sensitivity which can be described by the insulin concentration required for half-maximal effect (K_m); and/or to insulin responsiveness which is the maximal response to insulin (V_{max}). In order to define both the dose-response relationship and the maximum effect of insulin on glucose metabolism, at least three euglycemic clamps with different rates of insulin infusion were required in the same subject [27]. To simplify the procedure, Rizza et al. introduced a method to determine the insulin dose-response characteristics in a single clamp experiment [6]. Sequential infusions of insulin were used to raise the plasma insulin in a stepwise fashion; and each rate of insulin infusion was maintained for 2 hours. The glucose utilization determined during the last 40 minutes at each of the insulin infusion rates was plotted vs. the steady-state insulin concentration to yield the insulin dose-response curve.

Though insulin dose-response clamping can be employed to describe the kinetics of insulin sensitivity, the requirement of steady-state glucose and insulin levels may complicate the interpretation of the results, especially in the method of sequential insulin infusion. The insulin action on glucose metabolism is relatively slow and there was no actual steady-state glucose metabolism even over 5 or 8 hours of prolonged hyperinsulinemia plateau [91]. The approach of sequential

insulin infusion has been frequently used by other investigators [97, 98, 100]. Nosadini et al. infused insulin at four constant rates within 100 min [97]. In these studies, each steady-state hyperinsulinemia level was less than 2 hours, as a result, the glucose utilization measured at each insulin level may be affected by the previous insulin concentration. Whether the glucose metabolism represented the effect of prevailing or previous steady-state insulin levels was not clarified.

C. Sampling site

If the glucose concentration perfusing glucose-utilizing tissues (i.e., arterial glucose concentration) are matched, the glucose disappearance rates during a fixed rate of insulin infusion can be directly compared under various physiological conditions. Arterial sampling for determination of glucose concentration was employed in the early clamp development [62, 63, 64, 67]. To avoid the difficulty of arterial sampling, venous blood obtained from a dorsal vein of a heated hand (68 °C) was suggested by McGuire et al. [69]. The differences between arterial and venous kinetics of substances are due to 1) the transit times of substances through the circulatory paths between the two sampling site, and 2) the loss of substances to the intervening tissues [69]. By the heated vein method, the blood transit time was shorter (0.3 vs. 1.0 minute) and the glucose loss was reduced (1.9 vs. 2.9 % at basal insulin levels) compared to antecubital vein sampling [69]. This "arterialization" of venous blood using the warmed hand technique has been widely accepted with various temperatures employed ranging from 55 to 72 °C [6, 27, 70, 71, 72, 73, 97, 98].

Though the heated vein method provides a realistic alternative for blood sampling, the differences between venous and arterial kinetics cannot be completely eliminated. The venous blood transit time and irreversible glucose loss may be variability associated with the different temperatures applied for heating hands. Furthermore, the identical venous glucose concentrations may not represent the same arterial glucose levels if the insulin sensitivity is different. In the more insulin-sensitive subjects glucose utilized by tissues is greater, thus the difference of arterial and venous glucose concentrations is also greater. Under the identical venous glucose levels, the arterial glucose would be higher in a insulin-sensitive individual. This could result in overestimation of glucose disposal. Thus, although impractical in human studies, the arterial blood sampling gives more accurate estimations of insulin sensitivity.

D. Applications

The glucose clamp technique has been extensively applied to measure insulin sensitivity and/or β cell sensitivity to glucose in a variety of normal and pathophysiological circumstances. By this method, insulin resistance has been demonstrated in patient with type I diabetes mellitus [73, 74], type II diabetes mellitus [79], maturity-onset diabetes [70], uremia [67], obesity [27], aging [72], pregnancy and gestational-onset diabetes [71], hypertension [75], liver cirrhosis [76, 77], and hyperinsulinemia [78]. Recently, the glucose clamp has been developed in rats for *in vivo* estimation of insulin sensitivity under

anesthetized or conscious conditions [80 - 82]. Decreased insulin sensitivity measured by the clamp was reported in streptozotocin-induced diabetic rats [83], fructose-fed rats [84], sucrose-fed normal [85] and diabetic rats [86], human growth hormone (hGH)-treated rats [87]. Glyburide administration in normal rats [88] and vanadate treatment in diabetic rats [89] demonstrated increased insulin sensitivity as assessed by the clamp.

E. Assumptions

Several assumptions were made during the development of the clamp technique. They are briefly discussed below.

1) The metabolism of exogenous insulin is assumed to be indistinguishable from that of endogenous insulin [62]. The biological effect of exogenous insulin (usually porcine insulin) is possibly different from that of human insulin because of the structural variation. Concomitant with endogenous insulin secretion, a small percentage of proinsulin is released which is biologically less potent than insulin and not distinct from insulin by radioimmunoassay. In the hyperglycemic clamp in which the endogenous insulin is measured, the existences of proinsulin may result in an underestimation of insulin action.

2) When a constant level of insulin is obtained, there is presumably a steady-state of glucose metabolism. The plasma steady-state insulin will be achieved within 30 minutes after insulin infusion, while the

effect of elevated insulin on glucose metabolism is a much slower process [62]. The effect of insulin on glucose uptake is not directly related to insulin in the plasma pool, but is associated with insulin in an extra-vascular compartment which equilibrates slowly with the plasma pool [62]. The establishment of a relative steady-state in insulin action is related to the time required to achieve equilibration between plasma and extra-vascular insulin compartment.

Euglycemic clamp studies were performed by Doberne et al. to investigate whether glucose utilization changed during the steady-state period [91]. With a fixed rate of glucose infusion and sustained hyperinsulinemic plateau (80 - 100 $\mu\text{U}/\text{ml}$), they observed a mean of 18 % decrease in plasma glucose concentration over 60 minutes of the 3rd hour of clamping. When the clamp was extended to 5 or 8 hours, the glucose metabolic clearance rate (MCR) continuously increased for 5 hours after the initiation of hyperinsulinemia (mean = 88 $\mu\text{U}/\text{ml}$), and slightly decreased thereafter. Therefore in their experiment, no actual steady-state of glucose utilization was achieved even over 8 hours of clamping.

3) The underlying mathematical assumption of M/I ratio as an insulin sensitivity index is that M is linearly related to I and there is no intercept of M on I [64]. This assumption may not be true as there was an intercept of M on I plotted by Bergman et. al. [46]. The insulin dose-response curve for overall glucose metabolism was measured by the steady-state glucose infusion rate (M) at the sequential insulin infusion [6]. M was plotted versus the corresponding insulin level (I), the resultant dose-response curve was sigmoidal with M increasing

steeply (almost linearly) at I from 28 ± 2 to 101 ± 4 $\mu\text{U/ml}$. With further increases in insulin concentration, M increased only slightly and saturated at insulin levels between 200 and 700 $\mu\text{U/ml}$ [6]. In the euglycemic clamp, as the insulin plateau is kept approximately 100 $\mu\text{U/ml}$, M is almost linear to I. When insulin approaches the saturate value of the insulin dose-response curve, it is inappropriate to calculate the M/I ratio as insulin sensitivity index.

4) The use of clamp technique to assess insulin sensitivity assumes that non-insulin-dependent glucose uptake is unaffected by various pathophysiological states [64]. The amount of glucose required for maintaining steady-state glucose level (M) represents not only the insulin-dependent glucose uptake but also the effect of glucose on its own utilization. In normal individuals when euglycemia is kept and steady-state glucose concentrations are matched, the non-insulin-mediated glucose uptake should be similar. While in the insulin resistant subjects, relatively more of the non-insulin-mediated effect may contribute to M since the insulin action on glucose metabolism is diminished.

A recent study by Edelman et al. was conducted to define the insulin-mediated glucose uptake (IMGU) and non-insulin-mediated glucose uptake (NIMGU) in humans [92, 93]. Somatostatin was infused in stepwise manner to inhibit the endogenous insulin secretion. Either with or without replacement of exogenous insulin ($40 \mu\text{U}\cdot\text{m}^2\cdot\text{min}^{-1}$), whole body glucose uptake was measured at four glucose levels (4.5, 9, 12, 21 mM; i.e., 81, 162, 216, 378 mg/dl) to study IMGU and NIMGU. NIMGU was

determined by glucose uptake during somatostatin-induced insulinopenia (no insulin replacement). IMGU was calculated by subtracting NIMGU from glucose disposal rate (GDR) during hyperinsulinemia (460 pM; i.e., 54 $\mu\text{U/ml}$), that is, $\text{IMGU} = \text{GDR} - \text{NIMGU}$. Their studies suggested that NIMGU, IMGU, and whole-body GDR, were increased with the levels of serum glucose and were non-linear to the glucose concentrations being studied [92].

5) The rate of glucose utilization (corrected by urine loss) under steady-state is presumed to be equal to the sum of glucose infusion rate and the rate of endogenous glucose production as determined by tracer methodology [46]. The labeled glucose molecule is assumed to be biologically and metabolically indistinguishable from unlabeled glucose [94]. [$3\text{-}^3\text{H}$]glucose given in a primed continuous fashion has been extensively applied to estimate endogenous glucose production (R_a). The primed dose was usually 25 μCi and the constant infusion rate was often 0.25 $\mu\text{Ci/min}$ [27, 67]. During the steady-state, the glucose appearance (both endogenous and exogenous) should equal to the glucose disappearance, i.e., $R_d = R_a + \text{GINF}$.

However, the clamp data of Rizza et al. [6] as replotted by Bergman et al. [46] suggested that at high rates of exogenous glucose infusion (GINF) the calculated glucose production (R_a) was significantly negative. Many other investigators have reported the negative values of R_a determined by the tracer method [95, 96, 97, 98]. Negative values of R_a were usually considered to represent complete suppression of glucose

production [92, 94, 95], however, this results in an underestimation of hepatic glucose production as well as the glucose uptake.

The physiologically impossible negative numbers obtained for hepatic glucose production with tracer methodology may be due to 1) the difference in the metabolism of glucose tracer compared with unlabeled glucose, i.e., apparent isotope discrimination [99], 2) insufficient modeling of glucose kinetics which is assumed to be one-compartment with a fixed-pool volume [99], and 3) a contamination in the tracer preparation. The presence of a contamination or an isotope effect was demonstrated by comparing [3-³H]glucose with other tracers (6-¹⁴C]glucose and [2-³H]glucose [100]; or [6,6-²H₂]glucose [101]). However, insufficient modeling is thought to be more important. Addition of glucose tracer to the exogenous glucose infusate (hot GINF) during clamping yielded a more accurate Ra value which was not significantly less than zero and greater than that of cold GINF (no tracer in the exogenous glucose infusate) [94]. Employment of a one compartment model with a variable volume (regression approach) instead of the oversimplified fixed-pool model of glucose kinetics also improved the estimation of Ra [94, 99]. The hot GINF and regression methods provide an alternative for more accurate estimation of Ra by hyperinsulinemic-euglycemic clamp study.

The glucose clamp technique has provided an important tool to estimate insulin sensitivity, glucose production and utilization. With this approach the insulin action and glucose metabolism are determined under steady-state of glucose and insulin dynamics, and a number of

assumptions are made which may not be mathematically and physiologically correct. An alternative approach to assess glucose and insulin interactions in the non-steady-state is the minimal model of glucose kinetics.

(5). Minimal Model/FSIGT Technique

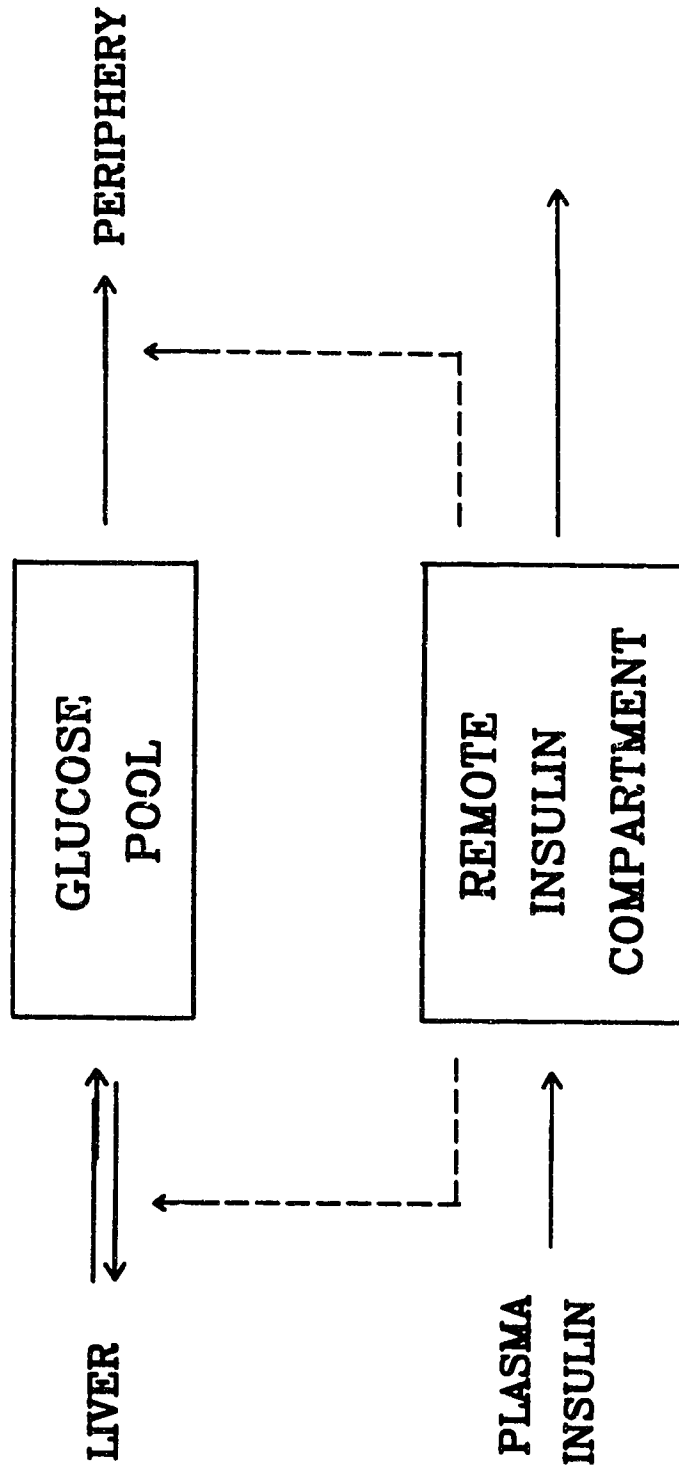
The minimal model of glucose and insulin kinetics, which was introduced and developed by Bergman and colleagues [102, 103] in the last decade, make it possible to quantify both insulin sensitivity and β cell sensitivity to glucose from a relatively simple glucose tolerance test, namely, the frequently sampled intravenous glucose tolerance test (FSIGT). In this paper the minimal model method will refer to the minimal model of glucose kinetics by which the insulin sensitivity and glucose effect on glucose disappearance can be determined.

A. Principle

The minimal-model method describes the glucose dynamics and the effect of insulin on glucose disappearance [Fig. 1]. In the glucose dynamic model, the extracellular glucose space is assumed to be a single, well-mixed compartment, and the rate of glucose disappearance is dependent on glucose itself, and on insulin in a compartment remote from the plasma. There are two differential equations of the model:

$$dG / dt = - [p_1 + X(t)] G(t) + p_1 G_b \quad (I)$$

$$dX / dt = -p_2 X(t) + p_3 I(t) \quad (II)$$



MINIMAL MODEL OF GLUCOSE DISAPPEARANCE

Fig. 1. Diagrammatic representation of the minimal model of glucose dynamics. The model assumes that the glucose space is a well mixed, single compartment, and the net rate of glucose disappearance from plasma is dependent on glucose itself and on insulin in a compartment remote from plasma.

where $X(t)$ = insulin in the remote compartment, p_1 = glucose disappearance term independent of insulin response, p_2 = insulin metabolism term of the remote compartment, p_3 = insulin distribution parameter, $p_1 G_b$ = net basal glucose production term. Equation I describes the change of glucose after a intravenous glucose injection which is dependent on 1) glucose itself at basal insulin, i.e., the effect of glucose on the net hepatic glucose production and on the glucose disposal to the periphery; and 2) the plasma insulin response, which augments the ability of glucose to clear itself from plasma. In the second equation, insulin action (X) is proportional to insulin in the remote compartment, most likely, the interstitial fluid.

The MINMOD computer program can solve the equations and define the parameters from the dynamics of plasma glucose and insulin during a single glucose tolerance test. Insulin sensitivity can be calculated from these parameters. The frequently measured plasma insulin and glucose concentrations from the FSIGT are submitted to a digital computer. Using the time course of plasma insulin concentration as input, the computer makes initial guesses of the parameters, solves the equations, and generates the glucose dynamics as output which is compared to the observed glucose data. Based on the initial results, the computer repeats this process continuously until the best parameter estimates are obtained, by which the model-generated glucose kinetics fits best to the original glucose data.

Glucose effectiveness (S_G): The model equation I states that the decline of glucose concentration in the plasma (glucose decline) after an i.v. glucose injection accounts for the glucose dependent component [$p_1G(t)$] and the component of the interaction of remote insulin and glucose [$X(t)G(t)$]. Therefore, $p_1G(t)$ reflects the glucose disappearance dependent on glucose and independent of the dynamic insulin response; the parameter p_1 is a measure of the ability of glucose per se to enhance its own disappearance independent of an increment in plasma insulin (glucose effectiveness), i.e., $S_G = p_1$.

Insulin sensitivity index (S_I): In the model insulin sensitivity is defined as the quantitative influence of insulin to increase the effect of glucose on its own disappearance [102]. From the minimal model, the insulin sensitivity index can be calculated as the ratio of p_3 to p_2 ($S_I = p_3 / p_2$), which is similar to the clamp-based insulin sensitivity. The model-estimated insulin sensitivity is analogous to the slope of the relationship between glucose infusion and the plasma insulin concentration, corrected for glucose level, during the euglycemic clamp [46]. S_I represents the sensitivity of both the liver and the periphery to dynamic insulin.

B. Remote insulin compartment

After the insulin appears in the plasma, sequential steps are required for the manifestation of insulin action on glucose metabolism, including the transport of insulin from plasma to cell surface, receptor occupation, activation of tyrosine kinase, translocation and activation

of glucose transporters, glucose phosphorylation and postphosphorylation metabolic events. In the minimal model, the concept of the remote insulin compartment is derived from the existences of a remote pool that is intimately involved in the action of insulin [104]. The studies of Andres et al. demonstrated that the extra-vascular insulin compartment, slowly equilibrated with plasma pool, correlated remarkably with the time course of glucose metabolism [62, 63]. They concluded that the slow equilibrating insulin compartment (rather than plasma insulin) was a more direct determinant of glucose utilization.

The remote insulin compartment was originally presumed to be related to binding of the hormone to receptor, insulin mediator, and other postreceptor events [105]. A recent study was carried out by Yang et al. to examine the relationship between transcapillary insulin transport and insulin action in dogs [106]. They reported that there was a remarkable similarity ($r = 0.95$) in the dynamics of insulin in lymph and glucose utilization (R_d), while only a modest correlation ($r = 0.78$) between R_d and plasma insulin. This intimate relationship between lymph insulin and R_d suggested that the transcapillary insulin transport is primarily responsible for the delay between changes in plasma insulin and changes in glucose disposal and may be the rate limiting step for insulin action [106]. There has been evidence that the movement of insulin across the capillary endothelial cells is a receptor-mediated process [107]; and sulfonylurea alleviates hyperglycemia in diabetes by preventing receptor down-regulation in endothelial cells [108]. In a perfused rat heart study, insulin binding to the capillary endothelial receptors appeared to be the central step in the transport of

intravascular insulin to cardiac muscle [109]. Therefore, the remote insulin compartment in the minimal model may largely reflect the insulin in the interstitial fluid; and the receptor-mediated insulin transport across capillary endothelium may contribute to the delay in insulin action.

C. Validation

The minimal model method has been validated against the glucose clamp technique for the measurement of insulin sensitivity. The insulin sensitivity index obtained from the minimal model (S_I) was highly correlated ($r = 0.82$, $p < 0.005$) with that from glucose clamp ($S_{I(\text{clamp})}$) in dogs [110]. A strong correlation ($r = 0.89$, $p < 0.001$) and similarity between S_I and $S_{I(\text{clamp})}$ were also demonstrated in normal man [111]. This relationship has been questioned since a weak correlation between S_I and $S_{I(\text{clamp})}$ was reported by Reaven et al. ($r = 0.44$, $p = \text{NS}$, [112]) and Beard et al. ($r = 0.54$, $p = 0.11$, [113]) in normal humans. Bergman et al. introduced a modified FSIGT protocol by the addition of tolbutamide at 20 minutes after the glucose injection and changed the sampling schedule, to improve the estimation of S_I [105]. The S_I determined from the modified protocol had a strong positive correlation ($r = 0.84$, $p < 0.002$) with $S_{I(\text{clamp})}$ [113]. The failure to obtain a good correlation between S_I and $S_{I(\text{clamp})}$ in some studies may be due to the difference between model-derived S_I and $S_{I(\text{clamp})}$, or that the inappropriate FSIGT protocol was used.

While the $S_{I(\text{clamp})}$ reflects the whole-body glucose disposal involving insulin-dependent and noninsulin-dependent glucose utilization, the model-based S_I accounts for the effect of insulin on glucose disposal (insulin-mediated glucose uptake) and on the suppression of hepatic glucose production. It should also be noted that clamp-derived non-insulin-mediated glucose uptake (NIMGU, [92, 93]) is not identical to S_G in the minimal model. NIMGU is the estimate of the glucose utilization with little or no insulin presented, whereas S_G is the measure of noninsulin-mediated glucose uptake in the presence of basal insulin concentrations.

The value of S_G estimated from the model was compared with a direct measurement where the endogenous insulin response was completely suppressed by somatostatin [122]. The pancreatic hormones were maintained at the basal level by intraportal replacement of insulin and glucagon. The S_G estimated from the model ($0.033 \pm 0.004 \text{ min}^{-1}$) was not significantly different from that estimated from the exponential rate of fall of plasma glucose in the absence of response insulin ($0.025 \pm 0.004 \text{ min}^{-1}$, $P > 0.25$). The value of S_G obtained from the tolbutamide modified protocol ($0.028 \pm 0.003 \text{ min}^{-1}$) was nearly identical to the directly measured value. These results suggested that the computer modeling approach is able to separate insulin-dependent and glucose-dependent glucose utilization from a single FSIGT experiment, and represented a direct confirmation of the minimal model.

The minimal model method has been applied to measure insulin sensitivity in various insulin-resistant states, such as obesity [103],

aging [114], HLA-identical nondiabetic siblings of IDDM patients [115, 116], prior gestational diabetes [117], and GH-treated dogs [118]. Modification of the FSIGT protocol by addition of either tolbutamide (TOLB) at 20 minutes or somatostatin (SRIF) at -1 minute can improve the estimation of insulin sensitivity in humans and dogs [119]. SRIF delayed insulin secretion without any change in magnitude and TOLB injection provoked an immediate secondary peak in insulin response, without directly affecting insulin sensitivity. Recently, the standard 180-min FSIGT protocol was modified for application in children by abbreviating the protocol to 90 minutes [120]. This abbreviated protocol was demonstrated to be a safe, accurate and valid technique for the estimation of S_I in children, and impaired insulin sensitivity was shown to exist at puberty and in obesity with this approach.

The minimal model / FSIGT protocol (either original or modified method) requires sufficient endogenous insulin secretion in response to secretagogues to allow for the estimation of insulin sensitivity. Yang et al. stated that the minimum integrated insulin of $1000 \mu\text{U}/\text{m}^2 \cdot \text{min}$ for the modified protocol and of $1500 \mu\text{U}/\text{m}^2 \cdot \text{min}$ for the original protocol was necessary for the reliable estimation of S_I or S_G [119]. In the insulin deficient states, it is not possible to determine S_I without the insulin response. With exogenous administration of insulin, Finegood et al. were able to apply FSIGT in IDDM patients to estimate insulin sensitivity [121]. S_I and S_G were not different from the exogenous insulin-modified and TOLB-modified protocol in normal subjects. Their results demonstrated that S_I was reduced in poorly controlled IDDM and

normalized in well controlled subjects, and S_G was decreased in all IDDM patients [121].

4. High fat diet and insulin resistance

High fat diet has been documented to induce insulin resistance and impaired glucose metabolism in rats both *in vivo* and *in vitro* (Table 1. and 2.). Various degrees of insulin resistance have been demonstrated in rats fed with high fat diet in which the fat content ranged from 50 % to 83.5 % in energy, for 5 days to 6 weeks. In the majority of the reports, saturated fatty acids (lard) were used in the high fat diet.

Feeding a high fat (67% of calories), carbohydrate free diet for 5 days to rats could cause a 50% decrease of insulin binding capacity in purified liver plasma membranes [123], and decreased insulin binding and glucose oxidation in response to insulin in rat adipocytes [124]. Kraegen et al. [21] reported that the rats fed with high fat (60% in calories) diet for 21-23 days displayed widespread but varying degrees of *in vivo* insulin resistance in peripheral tissues, with major effects in the principally oxidative skeletal muscles (soleus, diaphragm and red gastrocnemius).

5. Rationale

The minimal model/FSIGT method provides a new approach towards the *in vivo* quantification of insulin sensitivity independent of glycemia. From a single frequently sampled intravenous glucose tolerance test,

Table 1. The effects of short-term high fat diet on *in vivo* insulin action in rats

in vivo effects	start age or BWT	% fat* in diet	dietary term	reference
34% lower whole-body net glucose utilization	67-99 d	60	21-23 d	21
>50% reduction in net whole body glucose utilization	120-135 g	59	24 d	125
impaired glucose tolerance	weaning	67	5 wk	126
	100-120 g	66	3 wk	128
increased plasma glucose and FFA, decreased plasma insulin	60-70 g	67 or 83.5	3-5 wk	127
decreased glucose utilization in liver and adipocyte	100-120 g	66	2 wk	129
reduced metabolic index in muscle (14-56%), in WAT(27%), in BAT(76%)	67-99 d	60	21-23 d	21
decreased glucose turnover rate(79%)	weaning	70	4-6 wk	130
double SSPG level during SRIF, glucose and insulin infusion	67-99 d	60	21-23 d	21

*: Energy percentage of fat content in diet; BWT: body weight; WAT: white adipose tissue; BAT: brown adipose tissue; SSPG: steady-state plasma glucose; SRIF: somatostatin.

Table 2. The effects of short-term high fat diet on *in vitro* insulin action in rats

in vitro effects	start age or BWT	% fat* in diet	dietary term	reference
decreased glucose uptake in adipocyte	weaning	72	6 wk	131
	120-135 g	60	14 d	125
	115-135 g	60	10 d	132
	4 wk	70	7 d	133
	weaning	67 & 83.5	3-4 wk	134
	weaning	50	20-21 d	135
	115-135 g	60	10 d	132
	110-130 g	67	14 d	136
decreased glucose metabolism in adipocyte	100-120 g	67	5&10 d	124
	4 wk	70	7 d	133
	weaning	50	20-21 d	135
	weaning	67 & 83.5	3-4 wk	134
	115-135 g	60	10 d	132
decreased insulin binding in adipocyte	100-120 g	67	5&10 d	124
	120-135 g	60	14 d	125
	70-80 g	67	7 d	137
	115-135 g	60	10 d	132
	110-130 g	67	14 d	136
decreased insulin binding in muscle	120-135 g	60	14 d	125
	10 wk	67	10 d	138
reduced glucose uptake and metabolism in muscle	120-135 g	60	14 d	125
	10 wk	67	10 d	138
reduced insulin binding in liver	90-100 g	67	5 d	123
decreased insulin receptor kinase activity	110-130 g	67	14 d	136
decreased hepatic glucokinase activity	100-110 g	66	3 wk	128

*: Energy percentage of fat content in diet. BWT: body weight.

insulin sensitivity, glucose effectiveness, as well as, the β cell secretory function can be determined. As compared with the PST or glucose clamp methods, the minimal-model technique is relatively simple, less invasive, and less expensive to perform. The minimal-model allows for the estimation of insulin sensitivity from the dynamics of insulin and glucose following a glucose injection, whereas the clamp and PST require that the plasma insulin and glucose be held at steady-state for the estimation of insulin sensitivity.

The model-based approach does not require the same assumptions as discussed for the PST and clamp methods. These assumptions include that the plasma glucose and insulin reached steady-state during the clamp, that the linearity between steady-state glucose and insulin levels was held during PST, and that the non-insulin-mediated glucose uptake was not affected by various pathophysiological conditions in both PST and clamp. The model equations account for the kinetic parameters of the glucose and insulin dynamics rather than the absolute levels of glucose and insulin concentrations. However, the minimal model method does not allow the separated estimations of glucose production and utilization. The model approach relies on a fundamental assumption, that is, the kinetic model being used is physiologically realistic.

6. Research objectives

The clamp technique has been employed in rats to determine insulin sensitivity *in vivo*. No previous studies involving application of the minimal model to an FSIGT in rats has been reported. The current

investigations were carried out to 1) apply the minimal model to the rat model, and adapt and develop the FSIGT protocol in the rat; 2) modify the rat FSIGT protocol in order to improve the parameter estimation; and 3) examine the behavior of the modified method in a model of insulin resistance by measuring insulin sensitivity in insulin resistant rats induced by feeding a high fat diet. The final validation of the optimal FSIGT protocol will require direct comparisons with glucose clamp.

METHODS

Summary:

The frequently sampled intravenous glucose tolerance test (FSIGT) calls for a bolus of glucose and frequent blood samples. Additional injections were also required to modify the protocol. To conduct the FSIGT experiment on a conscious rat, two chronic cannula were implanted, one for injection of test substances and one for blood sampling. Two venous catheters, the inferior vena cava (IVC) and jugular vein (JV), were surgically implanted in each animal under general anesthesia. The cannula were then fixed on a pedestal located at the back of the neck for easy manipulation. After a week of recovery, the FSIGT experiment was performed on the conscious rat.

Details of the surgical procedures and general aspects of the FSIGT experiments are described in this section. The specific protocols for each group of studies performed are detailed in the Results section. Each specific protocol was designed according to the results from the previous set of experiments.

Surgical Preparation:

Cannula preparation Inferior vena cava and jugular catheters were surgically implanted at least 6 days prior to the performance of an FSIGT. For the IVC cannula, a 30 cm length of silastic tubing (0.020 inch ID x 0.037 inch OD) was bevelled at one end. A 3 mm long cuff of

silastic tubing (0.030 inch ID x 0.065 inch OD) was slipped over the catheter and placed 3.5 cm from the bevelled end. A 15 cm length of the same tubing was used for the jugular catheter with a similar cuff sitting 2.5 cm from the end. The catheters were packed individually and sterilized by gas sterilization.

Preparation of the pedestal The pedestal was made of two pieces of stainless steel tubing fixed on a polypropylene mesh. Stainless steel (23-gauge) tubing was cut into 2.5 cm pieces. Each piece of steel tubing was bent into a 90 degree right angle curve with two arms of 0.5 cm and 1.5 cm respectively. Two pieces of steel tubing were placed through a piece of polypropylene mesh (250 μ m hole size) in the same direction with the longer end vertical to the mesh surface and the short end parallel to the mesh. The steel tubing was fixed on the mesh by dental cement. The pedestal was sterilized in 70% ethanol and then rinsed in saline before implanting.

Surgical preparations The rat was anesthetized with 60-65 mg/kg sodium pentobarbital intraperitoneally (i.p.). Before the induction of anesthesia atropine 0.12 mg was injected i.p. Penicillin (44,000 IU) i.m. was administered to each animal. The back of the neck, the right jugular area and the central abdominal regions were shaved and swabbed with a Betadine solution. The surgical instruments were soaked in antiseptic solution (Hibidil 1:2000) and rinsed with saline before each surgery.

Jugular cannulation A 1 cm incision was made in the skin over the right jugular vein. The jugular vein was bluntly dissected and two anchor sutures (4-0 silk) were placed under the vein. The cannula was attached to a 23 gauge blunted needle and filled with heparinized saline (10 U/ml). The vessel midline was lifted slightly with Durmont forceps (blunt) and then punched using a 21 gauge needle until half of the bevelled end entered the lumen of the vein. The needle was quickly removed and the cannula was inserted. After the cannula was checked to ensure blood withdrawal was possible, two anchor sutures were tied around the cannula on either side of the cuff to prevent the catheter from slipping. The cannula was placed to avoid kinks and checked for patency with each step.

IVC cannulation A 3 cm incision was made in the abdominal midline starting approximately 1 cm below the xiphisternum. The gut was gently pulled out of the abdomen placed to the right and wrapped with a saline-wet sterile sponge. Special care was taken to avoid disturbing the ureter. Two anchor sutures (4-0 silk) were placed in the psoas muscle adjacent to the IVC. The cannula was attached to a syringe and then filled with heparinized saline. The midline of the vessel was lifted slightly and then punched with a 21 gauge needle so that half of the bevel entered the lumen. Immediately after the removal of the needle the bevelled end of the cannula was inserted into the vein directed proximally. Two sutures were tied around the vein on each side of the cuff. The cannula was positioned as a loop in the abdominal cavity to avoid kinks. Another suture was anchored in the abdominal wall about

1.5 cm from the right edge of the incision and tied around the cannula. The catheter was checked for patency after each step.

Installation of pedestal A transverse incision was made about 1 cm long at the back of the neck. Pockets were opened subcutaneously anterior and posterior to the incision using a pair of hemostats. Two holes were punched through the skin with a 19-gauge needle about 1 cm anterior to the incision. The pedestal tubing was poked through the holes made in the skin and the bulk of the pedestal was settled in the anterior pocket. The short ends of pedestal tubing were in the pocket parallel to the skin and the long ends of tubing were externalized. A short piece of PE50 tubing with a 1 cc syringe preloaded with heparinized saline was attached to the exteriorized pedestal tube, both PE50 and pedestal tubing were flushed to remove air. A silver probe (with eye) was passed subcutaneously from the site, at which the IVC cannula emerged from the abdomen, to the incision made at the back of the neck. The end of cannula was detached from the syringe and passed through the eye of the probe, and both the probe and cannula were pulled out at the neck incision. The jugular cannula was passed subcutaneously through the right side of the neck using the probe and exteriorized at the back incision. The cannula tubing was slipped over the pedestal tubing at the incision and secured by two sutures of 4-0 surgilene. The lines were cleared of blood or air, filled with heparinized saline, and positioned in the posterior pocket with no kinks. After the skin was closed, the PE50 line was folded over the tip of the pedestal tubing and capped using a 10 mm length of silastic tube. The rat was returned to a clean cage with paper towel as nesting material.

The rats were housed individually in plastic cages. The light cycle was fixed with lights on at 0700 and off at 1900 hr. Animals had free access to water and a standard chow diet (Wayne Rodent BLOX 8604).

FSIGT Experiment:

The first FSIGT experiment was performed 6-8 days after the surgery and there were 5-8 days between two experiments performed on the same animal. PE50 tubing was coiled over steam and soaked in 70% ethanol. The rat was placed in the experimental setting, a metabolic cage, 9 hrs before experiment (except for group 5 experiment, see Results) with free access to water, but no food. Before the experiment two pieces of coiled PE50 tubing were attached to a 23 gauge blunted needle with a syringe loaded with heparinized saline (10 U/ml), and flushed completely to remove any residual ethanol. The rat was placed on a towel and the pedestal caps were removed. The coiled PE50 tubing was connected to the steel tubing of the pedestal. After checking the patency of the line, the PE50 catheters were placed through the hole on the center of the metabolic cage cover. The blood sampling and injections were manipulated outside the cage without disturbing the animal. The rat usually moved around or rested quietly during the experiment.

Experimental protocol The jugular catheter was used for injections and the IVC cannula was used for blood sampling. A basal blood sample was taken at -5 or -2 minute, and glucose (300 mg/kg body weight) was given intravenously within 30 seconds beginning at 0 min. Blood samples

were frequently drawn over a varied period of time (see specific experiments) to define the glucose and insulin kinetics after the glucose bolus. The catheters were flushed with heparinized saline between samples. Blood samples were collected in heparinized microtubes containing sodium fluoride (heparin 10 U/tube, and sodium fluoride 0.75 mg/tube) and centrifuged for 3 minutes in a Beckman Microfuge. The plasma was transferred into microtubes and stored at -20°C for measuring glucose and insulin concentrations. The total blood loss was limited to less than 10 % of the whole blood volume of the animal. Specific protocols were modified by additional injections of somatostatin (SRIF) and tolbutamide (TOLB) or insulin.

Data Analysis:

The insulin and glucose time courses were submitted to the MINMOD computer program (Bergman, copyright RN, University of Southern California), and the parameters of insulin sensitivity and glucose effectiveness were estimated. Insulin area was calculated as the area under the insulin curve above basal, and K_G (glucose tolerance parameter) was expressed as the rate constant for the exponential glucose fall following a glucose injection (from 2.5 to 16 minutes). The data were statistically analyzed with student t-test, one-way and two-way analysis of variance where appropriate using MINITAB or SAS programs. The results were expressed as mean \pm SE unless otherwise indicated.

RESULTS

Overview of studies:

To determine the optimal protocol for estimation of insulin sensitivity and glucose effectiveness in the rat model, a sequence of specific protocols were undertaken. First, an FSIGT protocol with a glucose injection and only 7 to 8 samples was performed to adapt the technical details of performing an FSIGT to the rat model. Next, the protocol was modified by additional injections of somatostatin and tolbutamide. An effort was made to increase the number of samples for better definition of the glucose and insulin dynamics without further blood loss. Third, computer simulation was applied to determine the optimal protocol for parameter estimation from the four possible protocols. Finally, since the glucose plus tolbutamide protocol has been standardized in both human and dog and the glucose + insulin protocol was validated against the tolbutamide protocol in insulin deficient subjects, the glucose with insulin protocol was performed in the rat model. Animals were fed with standard chow diet and a high fat diet intended to induce insulin resistance. It was expected that insulin injection would be necessary for the determination of insulin sensitivity in the insulin insensitive animals. A range of insulin doses was applied in normal and high-fat-diet fed animals to determine the optimal dose for the estimation of insulin sensitivity.

Group 1. Glucose only protocols (GLU) in Long Evans (LE) rat

Hypothesis: An FSIGT experiment can be conducted in a conscious rat with chronic IVC and JY catheters. The minimal model of glucose kinetics can be applied to the dynamics of glucose and insulin in the rat model to estimate insulin sensitivity and glucose effectiveness.

Methods: Thirty-seven FSIGT experiments were conducted on 17 male LE rats with mean body weight of 360.7 ± 1.6 gram. The rat was transferred to a metabolic cage at 5 pm the day before the experiment to avoid excitement. Some food was left overnight and it was assumed that the rat would consume all the food by midnight.

After a basal sample collected at -5 min, glucose was injected at 0 min. Seven or eight blood samples (250 μ l each) were taken following one of four sampling schedules:

Protocol I: 2, 3, 5, 9, 16, 25, 35, 50 min;

Protocol II: 2, 4, 6, 10, 18, 23, 28, 35 min;

Protocol III: 2, 3, 7, 12, 20, 27, 31, 40 min;

Protocol IV: 2, 4, 8, 14, 22, 30, 45 min.

Results: The glucose and insulin dynamics after glucose injection are illustrated in Fig. 2. The four protocols (different sampling schedules) were combined to yield the mean time course of glucose and insulin concentrations. Considerable noise existed in both insulin and glucose curves when the four protocols were combined. Glucose and insulin were at their peak values at the first sample (2 min) after

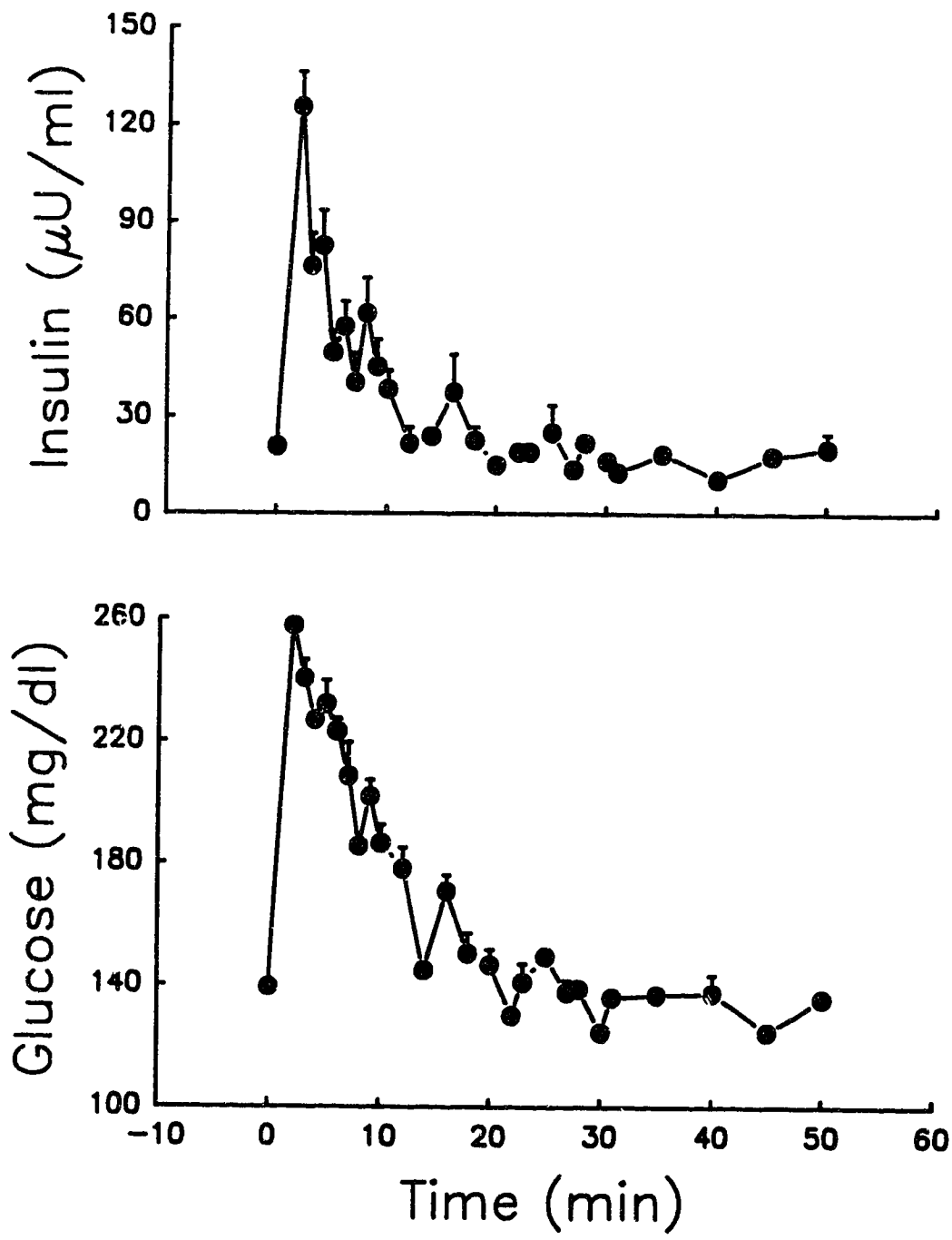


Fig. 2. The mean time course of glucose and insulin dynamics in Long Evans rats following a single glucose bolus at 0 minute. All of the data from the four sampling schedules were combined (protocol I, II, III, IV). The top panel shows the observed insulin and the observed glucose was plotted in the bottom panel.

glucose injection. The insulin level rapidly declined to basal prior to the glucose concentration.

The glucose and insulin kinetics from the individual protocols are plotted in Fig. 3. Insulin dynamics appeared to have greater variation among protocols than glucose kinetics; when the glucose time course was plotted as the difference between each glucose value and its basal concentration, the variation in the glucose curves was markedly reduced.

Table 3 lists the basic characteristics of the glucose and insulin dynamics of the four protocols. One-way analysis of variance was carried out for the statistical analysis. Body weight, basal insulin, and insulin areas were not significantly different between the four protocols. Basal glucose and K_G (rate of glucose disappearance) were significantly different. This difference might be due to the fact that the fasting period was not held constant for each experiment, and/or the sampling schedules applied may not sufficiently describe the glucose dynamics.

An example of a single FSIGT experiment and its model fit is shown in Fig. 4. The observed insulin is plotted in the top panel, the observed glucose concentrations and computer-derived model fit of glucose dynamics are represented in the lower panel. The observed glucose and insulin values were plotted as closed circles. In the lower panel, the solid curve gives the computer generated model-fit and the dashed line is the basal level of plasma glucose. The insulin sensitivity index (S_I), glucose effectiveness (S_G) and their respective

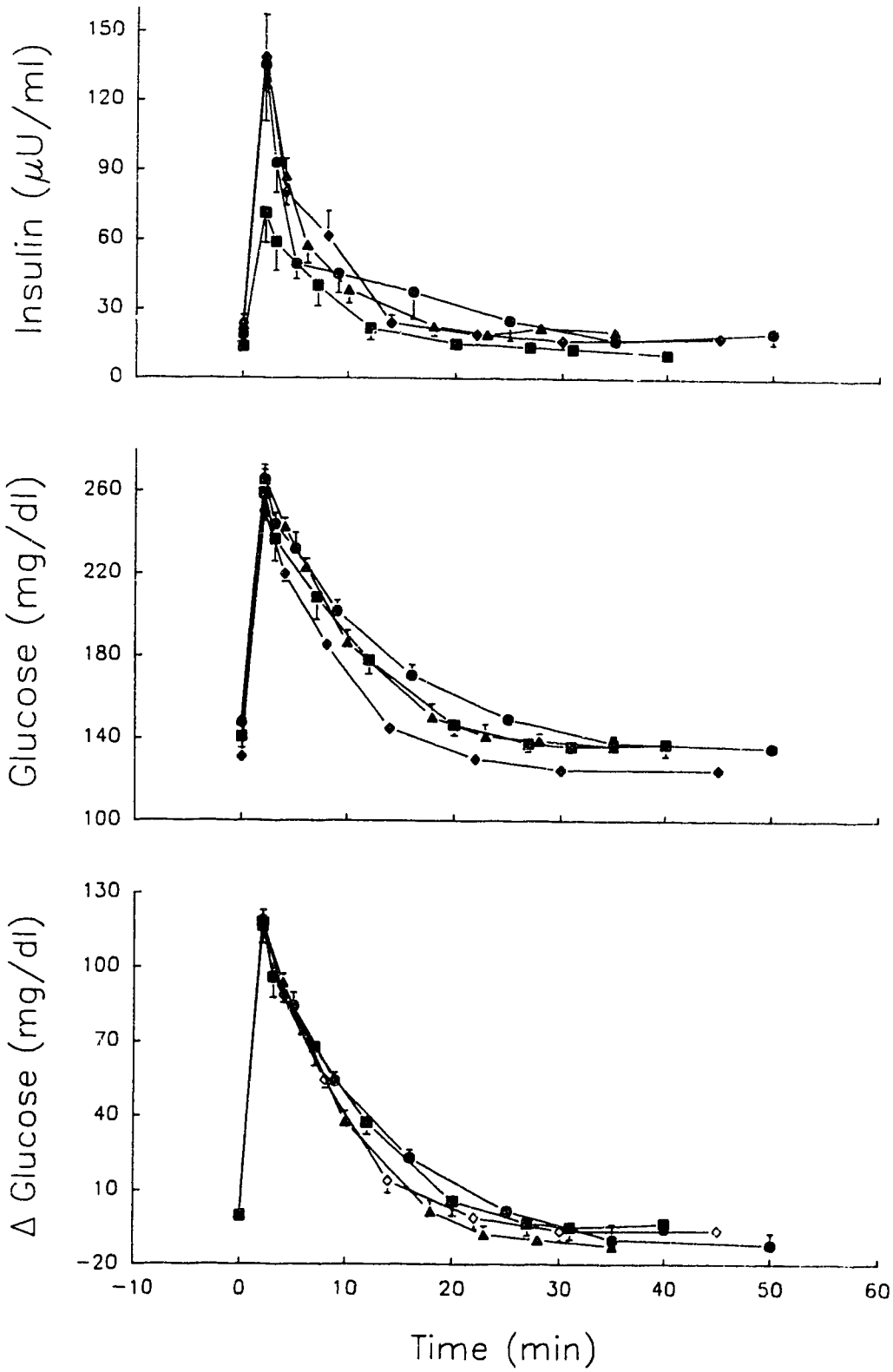


Fig. 3. The glucose and insulin dynamics of {GLUCOSE} protocols in LE rats. Closed circles, protocol I; filled triangles, protocol II; filled squares, protocol III, and filled diamonds, protocol IV. The observed insulin and glucose were plotted in the top and middle panels respectively. The Δ Glucose in the bottom graph was calculated as the difference between measured glucose and the basal glucose concentration (measured glucose - basal glucose).

Table 3. Data of {GLUCOSE} protocol in Long Evans rat FSIGT.

	Protocols				P*	Mean
	I	II	III	IV		
N	7	7	7	16		37
BWT(g)	366±15	349±17	350±13	368±13	>0.1	361±8
Basal GLU	148±3	149±3	141±6	131±3	<0.01	139±2
Basal INS	19±2	23±3	14±2	24±4	>0.1	21±2
KG(%)	3.71±.20	4.43±.28	3.51±.21	4.46±.27	<0.025	4.14±0.15
INS Area(μU/ml.min):						
Total	38±6	43±5	28±4	33±4	>0.1	35±15
>SS	22±5	20±3	15±3	16±3	>0.1	18±2

*, P values were calculated from one-way analysis of variance testing differences among the four protocols. N is the number of experiments in each protocol; BWT is the body weight in grams; Basal GLU is the basal glucose in mg/dl; Basal INS is the basal insulin in μU/ml; INS Area Total is calculated as the area under the insulin curve, and the INS Area >SS is the insulin area above steady-state.

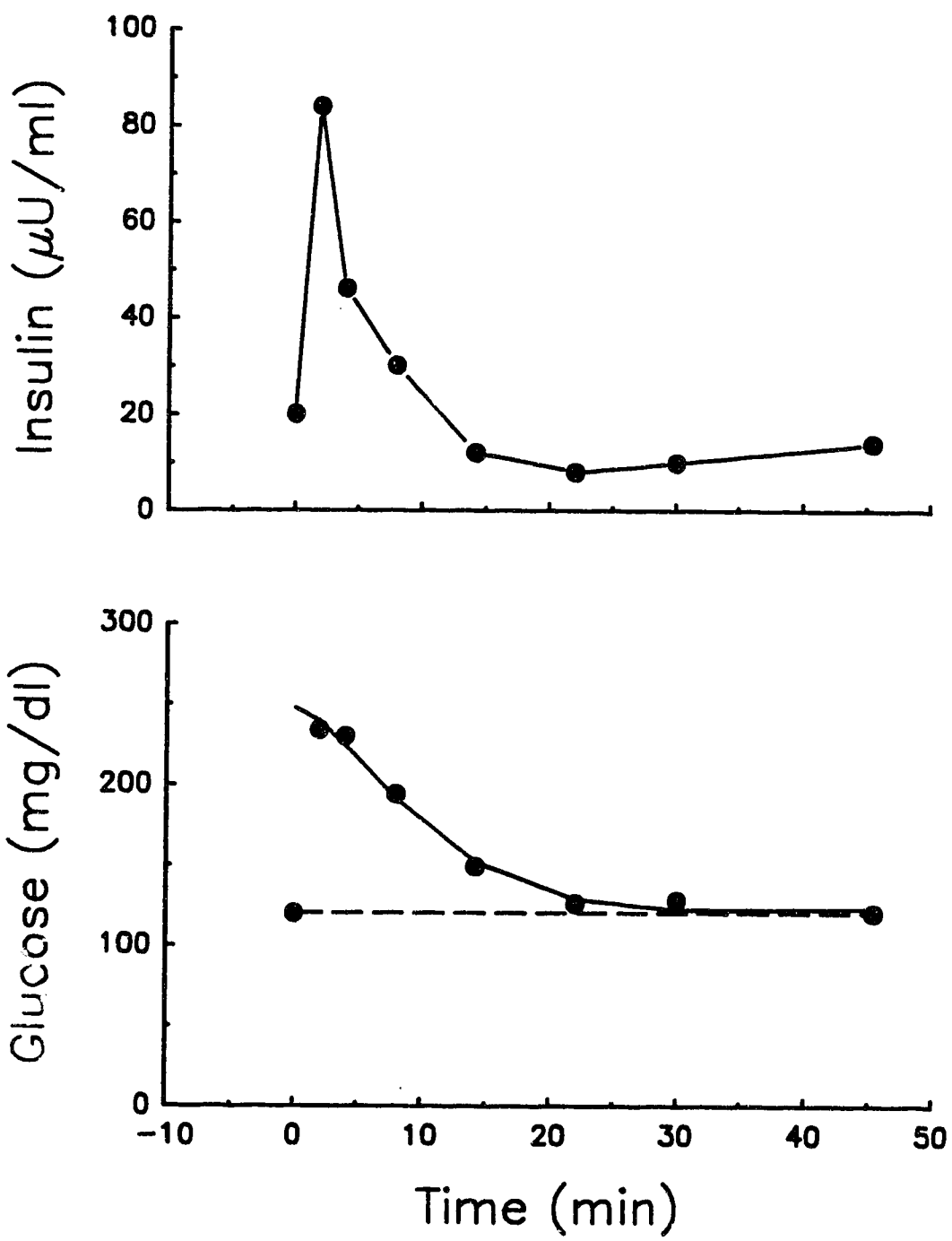


Fig. 4. An example of rat FSIGT ({GLUCOSE} protocol) with 8 samples. Glucose was injected at 0 minute. In the bottom graph the closed circles give the observed glucose values, while the solid curve is the calculated model fit of glucose dynamics by the computer MINMOD program. The dashed line shows the basal level of plasma glucose.

fractional standard deviations (FSD) from the model estimation are listed in Table 4. The FSD of the model parameter quantifies the certainty of the parameter estimate. In this paper I use the term "identifiability" to refer to the ability of the MINMOD computer program to obtain estimates of the model parameters from a given set of data. A data set is considered identifiable if the FSDs for all four parameters are less than 100 %. The data set is considered non-identifiable if any FSD exceeds 100 %. In this set of experiments in which only glucose was injected and 7 to 8 samples were taken, the identifiability was only 43% (16 out of 37).

Conclusions: From the group 1 study, we concluded that it was possible to perform an FSIGT experiment in the rats with the current techniques. Insulin sensitivity and glucose effectiveness could be estimated from an FSIGT performed in rats with only seven or eight blood samples. The poor identifiability and high FSD suggest that the protocol is not adequate to describe the dynamics of insulin and glucose, and thus modifications of the protocol were required for better estimation of parameters.

Group 2. Glucose combined with SRIF and TOLB protocols in LE rat

Hypothesis: Modification of the protocol by additional injections of somatostatin and tolbutamide can improve the model parameter estimates and decrease fractional standard deviations.

Somatostatin, or somatotropin releasing inhibiting factor (SRIF), is

Table 4. Parameters of {GLUCOSE} protocol in LE rat FSIGT.

	Protocols				P*	Mean
	I	II	III	IV		
S_I	3.34	13.41±3.22	7.78	7.66±1.00	0.18	8.84±1.61
FSD(%)	7	19±2	8	15±3	0.45	15±2
S_G	3.17	5.26±0.76	5.78	9.69±1.06	0.033	7.69±0.90
FSD(%)	18	45±9	34	18±4	0.015	27±5
Identify	1/7	4/7	2/7	9/16		16/37

*, P values were calculated from one-way analysis of variance testing the four protocols. S_I , $\times 10^{-4} \text{ min}^{-1}/(\text{uU/ml})$; S_G , $\times 10^{-2} \text{ min}^{-1}$. The identify is the number of identified experiments (the FSD of parameter estimation less than 100%) over the total experiments.

secreted by the hypothalamus, as well as, by pancreatic islet D cells. It is known to inhibit the release of insulin and glucagon from the β and α cells. Tolbutamide (TOLB) is a sulfonylurea which is known to augment insulin secretion. By giving SRIF just before glucose and TOLB during the glucose decline, the dynamics of insulin secretion could be changed such that the initial insulin release evoked by the glucose challenge is diminished and the peak concentration of insulin is delayed so that it now occurred in the middle of the glucose decline.

Methods: Eleven FSIGTs, {SOMATOSTATIN + GLUCOSE + TOLBUTAMIDE} (SGT) protocol, were performed on 6 male LE rats with average body weight of 296.3 ± 6.8 gram. The food was removed at midnight so that the rat was fasted for 9 hrs before the experiment. After a basal blood sample, SRIF ($16 \mu\text{g}/\text{kg}$) was injected at -0.5 min before the glucose given at 0 min. TOLB ($3.5 \text{ mg}/\text{kg}$) was given at 8 min. Eight blood samples ($250 \mu\text{l}$ each) were taken after the glucose load according to one of the following sampling schedules:

Protocol Ia: 2, 3.5, 6, 9, 11, 14, 20, 30 min;

Protocol IIa: 1.5, 3, 5, 7, 9.5, 12, 16, 25 min;

Protocol IIIa: 2, 4, 6.5, 9, 10, 13, 20, 35 min.

Results: The three protocols of SGT were combined, and the mean insulin and glucose concentrations are plotted in Fig. 5. The initial insulin secretion was markedly (though not completely) suppressed by SRIF, and the insulin peak followed the injection of TOLB. As a consequence, the rate of initial glucose disposal was slightly reduced and then the rate of glucose disappearance was augmented by insulin. Therefore, as

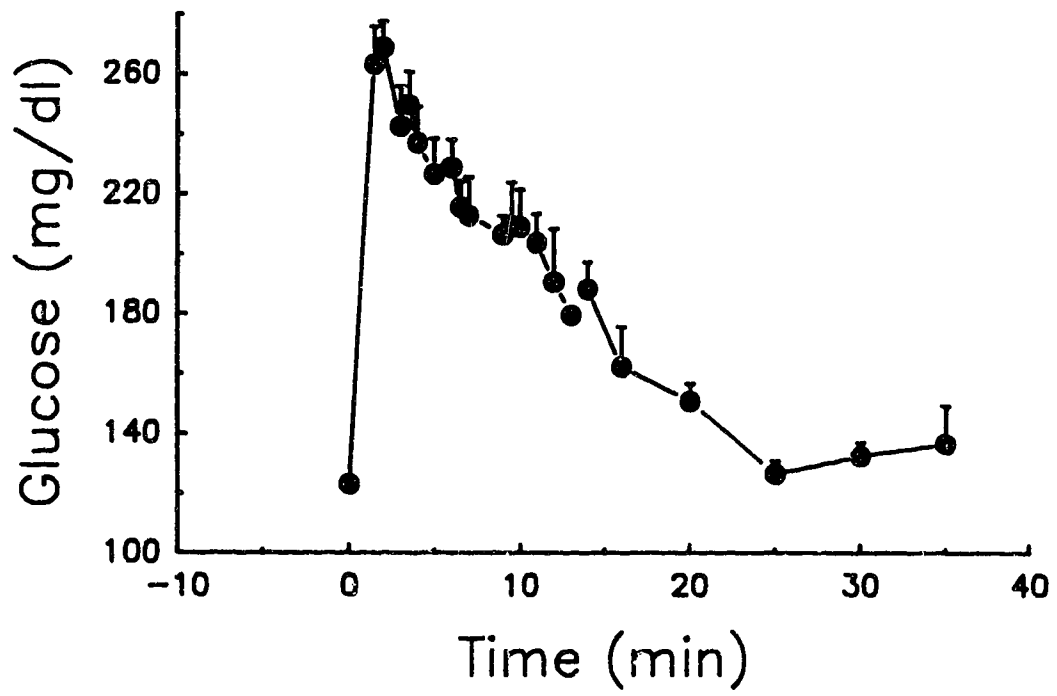
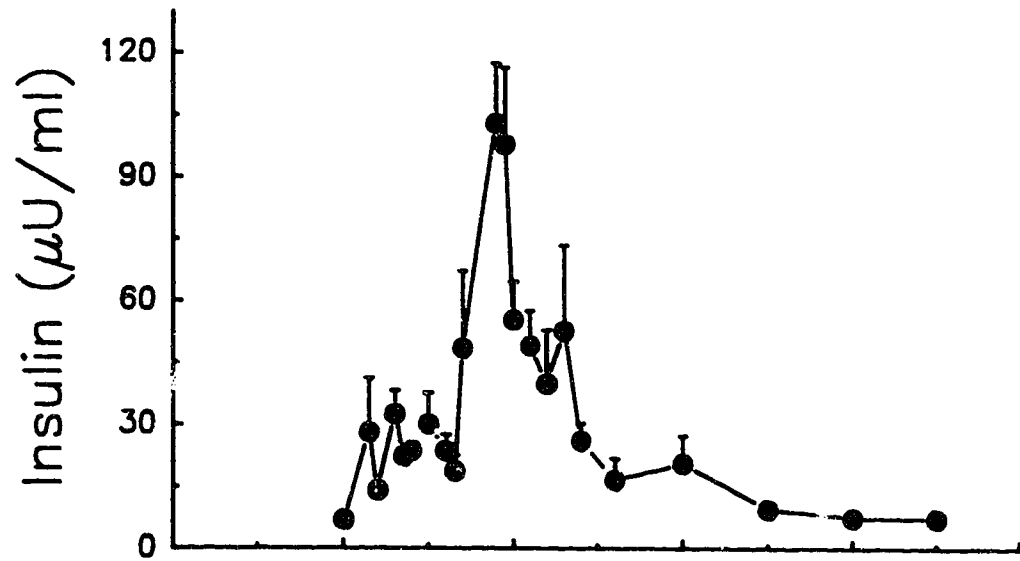


Fig. 5. The mean glucose and insulin kinetics of {SOMATOSTATIN + GLUCOSE + TOLBUTAMIDE} protocols. The initial insulin response was suppressed but not completely by somatostatin injection. The insulin peak evoked by tolbutamide was approximately $100 \mu\text{U}/\text{m}^3$

compared with the {GLUCOSE} protocol, the early glucose decline was dependent more on glucose itself at basal insulin rather than on both incremental glucose and insulin.

The SGT protocol was compared with the {GLUCOSE} protocol (Table 5). The two sets of experiments were not conducted on the same group of animals. The fasting time for the SGT experiments was relatively constant since the food was removed at midnight. The difference in the basal glucose, basal insulin and K_G between the two protocols might be due to the variation in the animal's body weight and uncontrolled fast time in the two protocols. Despite the delay of insulin peak in the combined protocol, the total and above steady-state insulin area were not different. The estimation of S_I was not improved by the modified protocol. FSD for S_G was lower in the combined protocol though the difference did not reach statistical significance. However, the ability of the model to identify parameters was markedly increased from 43% in glucose only protocol to 73% in the combined protocol.

The original FSIGT protocol (Glucose injection only) was modified by additional injections of somatostatin prior to glucose and tolbutamide at 8 minutes after glucose load (SGT protocol). Though the modified protocol improved the ability of the model to estimate parameters of glucose dynamics, the FSD for both S_I and S_G were not significantly reduced in the modified protocol. To enhance the identifiability and accuracy of parameter estimation by the model, more data points were desirable to better define the glucose and insulin dynamics. Furthermore, since the comparison of protocols was made on two separate

Table 5. Comparison of {GLUCOSE} and modified protocols in LE rat FSIPT

	GLUCOSE	SRIF+GLU+TOLB	p*
N	37	11	
BWT(g)	361±8	296±7	0.0001
Basal GLU(mg/dl)	139±2	123±3	0.0012
Basal INS(μU/ml)	21±2	7±0.6	0.0003
KG(%)	4.14±0.15	3.37±0.26	0.01
INS Area(μU/ml.min):			
Total	35±15	32±5	0.55
>SS	18±2	14±2	0.33
S _I	8.84±1.61	11.07±1.57	0.41
FSD(%)	15±2	16±3	0.78
S _G	7.69±0.90	5.13±0.82	0.093
FSD(%)	27±5	13±4	0.088
Identify	16/37(43%)	8/11(73%)	

*, P is calculated from student t test.

groups of rats, it was deemed necessary to perform the different protocols in the same group of animals.

Conclusions: The modified SGT protocol resulted in an increase of the parameter identifiability, despite the fact that the FSD for S_1 estimation was not improved.

Group 3. FSIGT experiment in the Sprague-Dawley (SD) rat

Hypothesis: By increasing the number of samples, the measurement of model parameters should be improved.

The first two groups of studies were performed in Long Evans rats because we were borrowing instruments and learning surgical techniques from Dr. Susan Jacobs. Subsequently we were able to purchase tools and conduct the animal surgeries in our laboratory, so we switched to male Sprague Dawley rats since glucose metabolic studies have been usually carried out on SD rats rather than on LE rats.

Methods: Direct comparison of two types of protocols in the same group of animals was set up to allow for an unbiased assessment of the two protocols. {GLUCOSE} protocol and SGT protocol were performed in a randomized order in a group of SD rats. A total of 27 experiments were completed on 8 male SD rats with average body weight of 357 grams. The animals were fasted for 9 hours in the experimental setting before the FSIGT. The experimental procedure was according to one of the two protocols. *Protocol A* (GLUCOSE, n=13): glucose was injected at 0 min,

150 μ l blood samples were taken as the following schedule: -2, 2, 3, 4, 5, 6, 8, 10, 14, 18, 23, 28, 34, 40 min. *Protocol B* (SGT, n=14): SRIF (16 μ g/kg) was given at - 0.5 min prior to glucose injection (0 min), and TOLB was injected at 8 min. Samples (150 μ l) were drawn according to the following schedule: -2, 2, 4, 7, 9, 10, 11, 12, 15, 18, 23, 34 min. Additional blood samples (80 μ l) were taken at 3, 5, 6, 40 min for glucose measurement only, so that the number of data points for glucose analysis could be increased to allow for a better description of the glucose kinetics.

Results: Fig. 6 illustrates the mean time courses of insulin and glucose dynamics in {GLUCOSE} and {SGT} protocols. In {SGT} protocol, the rate of glucose clearance was initially slightly lower as the consequence of suppression of initial insulin secretion, and then was augmented with the appearance of insulin peak following TOLB injection. Although the time course of glucose decline was different between the two protocols, the overall glucose tolerance (K_G) was not significantly different ($P=0.25$).

The mean S_I , S_G , and their FSD were plotted for each protocol (Fig. 7). Insulin sensitivity was not different between protocols; whereas S_G as determined by the {SGT} protocol was lower than that using the {GLUCOSE} protocol ($P = 0.0087$). The FSD was markedly reduced for both S_I ($P < 0.0001$) and S_G ($P = 0.015$) in the {SGT} protocol. Furthermore, the percentage of identifiable experiments was 84.6% (11/13) for {GLUCOSE} protocol and 92.9% (13/14) for SGT protocol. If the criteria for identifiability were increased to require that the FSDs of both S_I

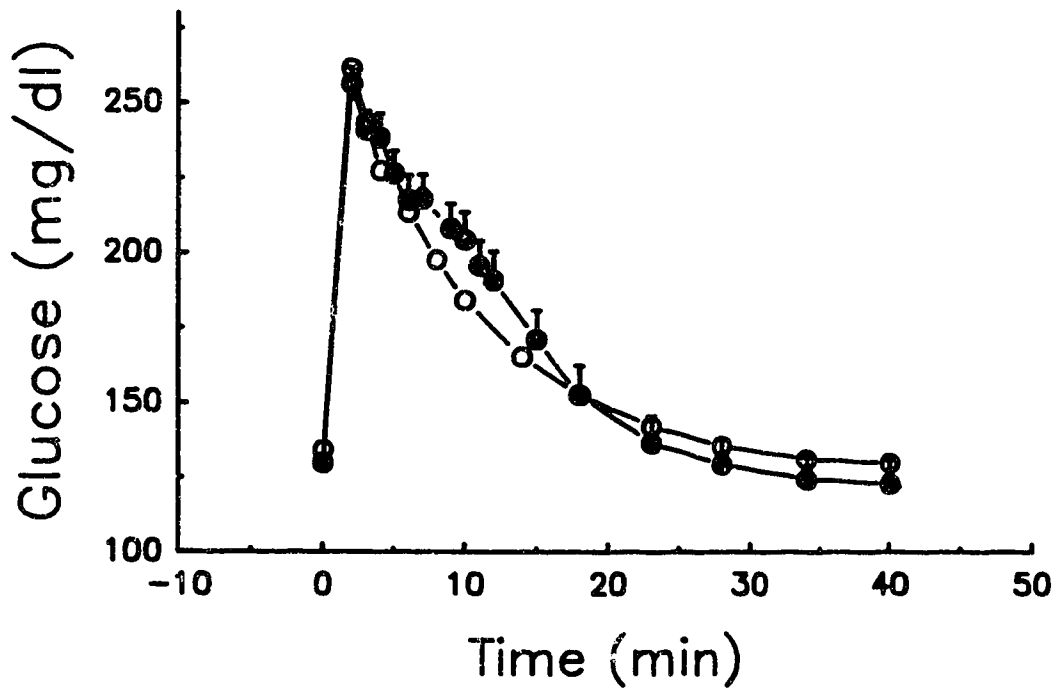
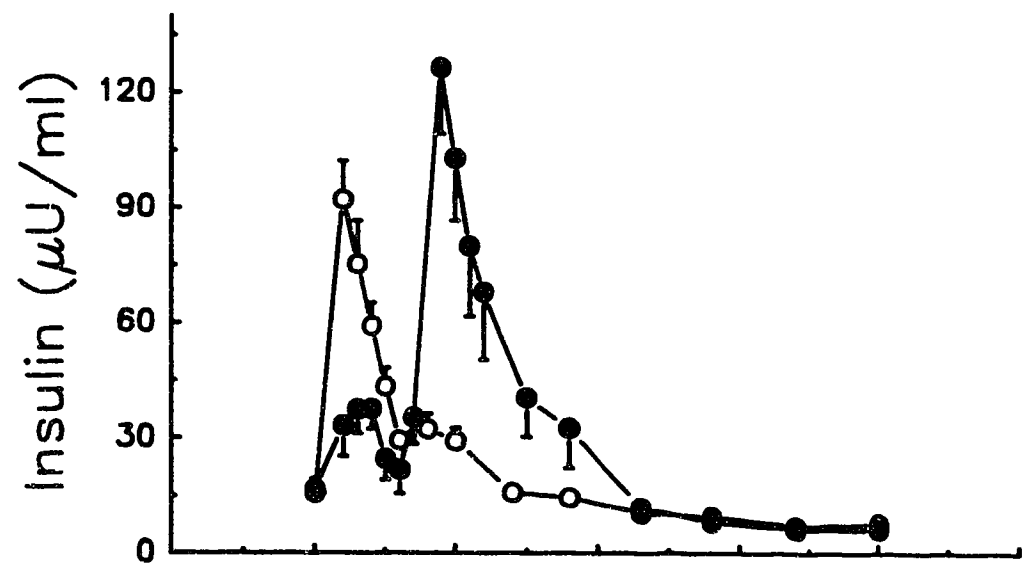


Fig. 6. The glucose and insulin dynamics in Sprague-Dawley rat. The {GLUCOSE} protocol was given in open circles and the modified protocol ({SOMATOSTATIN + GLUCOSE + TOLBUTAMIDE}) was shown in filled circle. Given the partial suppression of initial insulin response, the rate of glucose disappearance rate (K_G , from 2 to 16 minute) was not significantly different ($p = 0.25$).

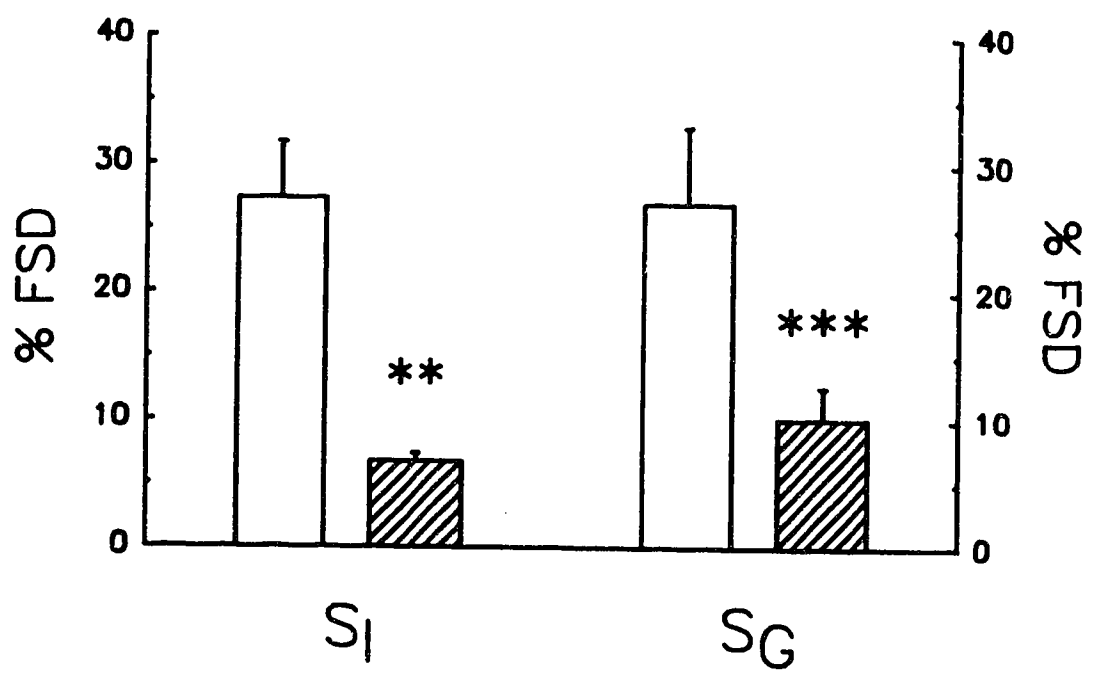
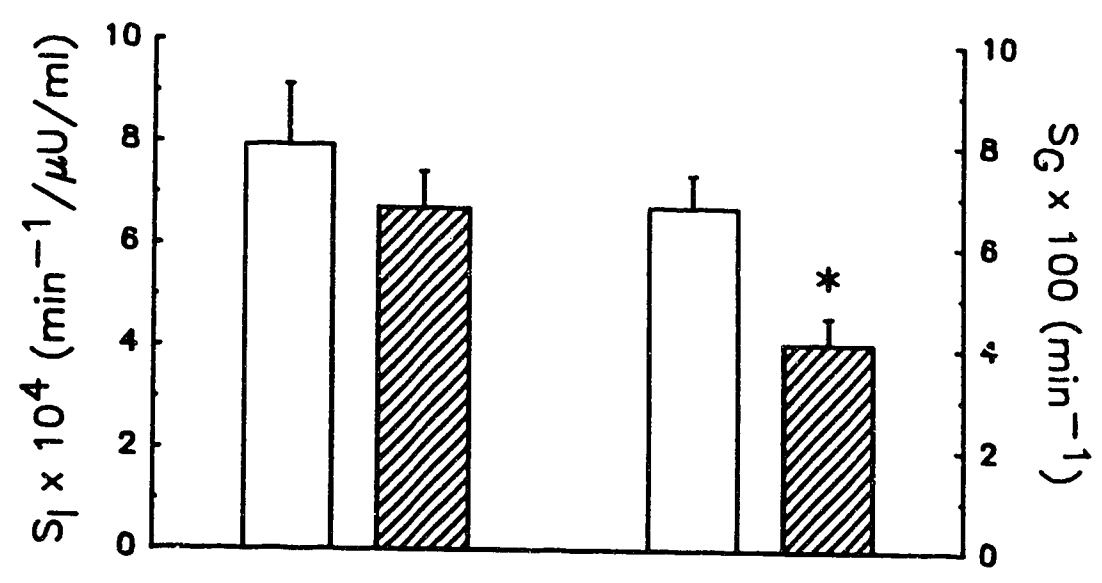


Fig. 7. The parameters of FSIGT in SD rat. Protocol A ({GLUCOSE}) was plotted in open boxes, and protocol B (modified protocol) was shown in hatched bars. The mean values of S_I and S_G were given in the upper panel, and the lower panel gives their fractional standard deviations. Student t test was performed in comparison of the means. *, $p = 0.087$; **, $p < 0.0001$; and ***, $p = 0.015$.

and S_G were less than 15%, the identified experiments were 1/14 in protocol A and 12/14 in protocol B.

Conclusions: Direct comparison of the two protocols suggests that the modified {SGT} protocol results in more reliable and accurate estimations of S_I and S_G . With more blood samples to describe the glucose and insulin dynamics, the parameter estimation and the model identifiability was improved.

Group 4. Simulation

Hypothesis: Given well defined glucose and insulin dynamics (25 samples), the computer simulation can determine the best protocol(s) from the four given protocols: {GLUCOSE}, {SOMATOSTATIN + GLUCOSE} (SRF), {GLUCOSE + TOLBUTAMIDE} (TOL), and {SOMATOSTATIN + GLUCOSE + TOLBUTAMIDE} (SGT).

Methods: Computer simulation was carried out to determine the best FSIGT protocol. The procedure is as outlined in Figure 8. The simulation process was performed as follows: 1) An insulin profile and a set of parameters were submitted to a program to generate a "perfect" glucose dynamic, 2) A specified level of random error was added to the perfect glucose to obtain an "experimental" glucose pattern, 3) The insulin and glucose profiles were entered to the MINMOD program for parameter estimation, and 4) The estimated parameters were compared with the given parameter set.

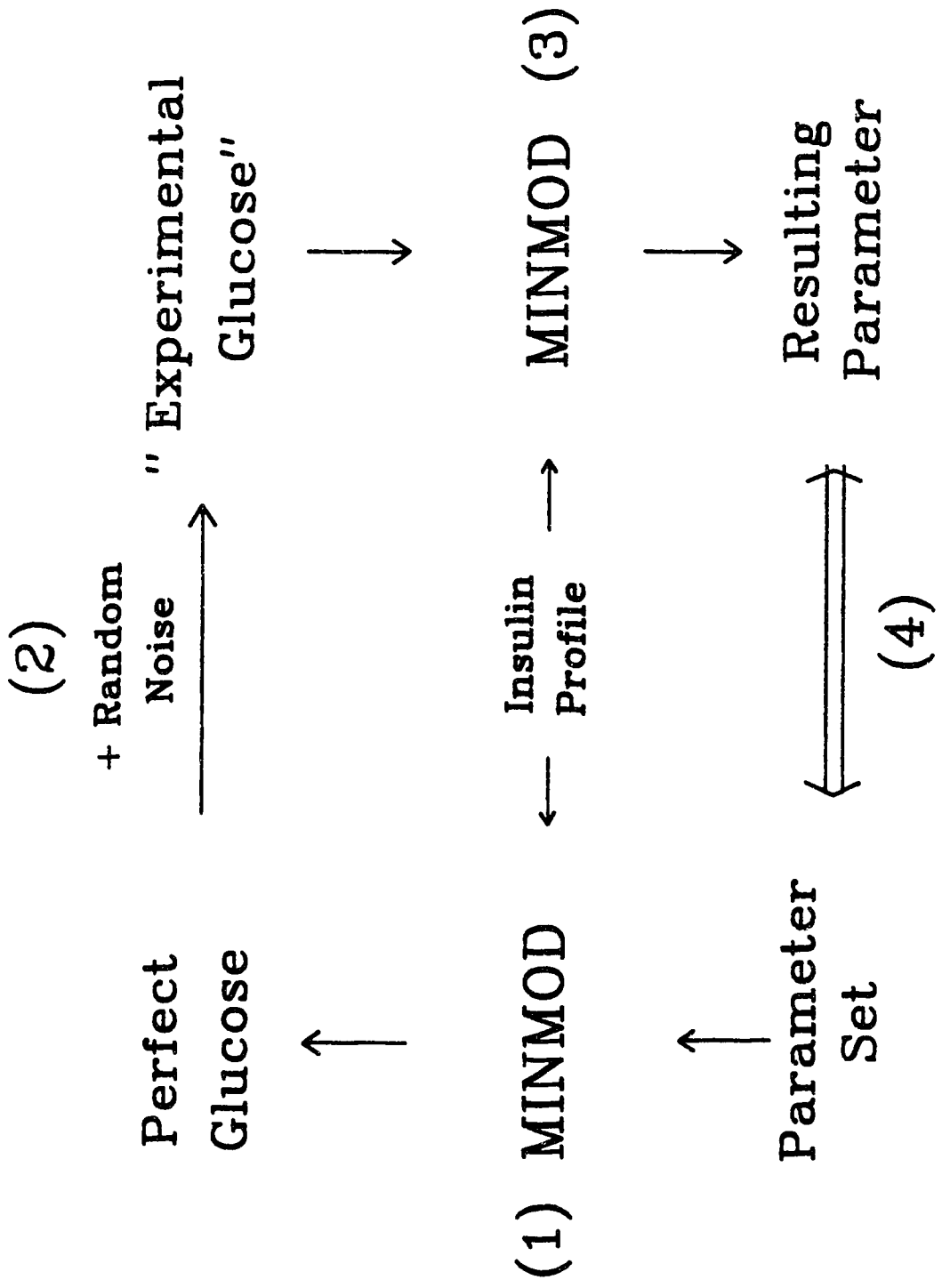


Fig. 8. Schematic of the simulation process. The parameter set obtained from preliminary experiments and an insulin profile were submitted to the MINMOD program, and the computer generated the "perfect glucose" dynamics. Random error was added to the perfect glucose, which resembled the experimental uncertainty, to yield the "experimental glucose". The generated experimental glucose and the insulin profile were entered to the computer program, and the parameters of the model were estimated. The resulting parameters were compared with the given parameter set by calculating their means and standard deviations.

Twenty-five data points were generated for each glucose pattern so that the glucose kinetics were well described. For a given set of parameters and an insulin profile, the addition of random error (3%) to the perfect glucose dynamics was repeated 100 times to create 100 glucose patterns. Four insulin profiles corresponding to four specific protocols were tested (Fig. 9): {GLUCOSE}, {GLUCOSE + TOLBUTAMIDE}, {SOMATOSTATIN + GLUCOSE}, and {SOMATOSTATIN + GLUCOSE + TOLBUTAMIDE}. For each insulin pattern, four sets of parameters were assigned to the computer simulation: (1) $S_I = 7.5 \times 10^{-4} \text{ min}^{-1}/\mu\text{U/ml}$, $S_G = 7.1 \times 10^{-2} \text{ min}^{-1}$ (normal S_I and S_G); (2) $S_I = 7.5$, $S_G = 3.5$ (normal S_I and low S_G); (3) $S_I = 3.75$, $S_G = 7.1$ (low S_I and normal S_G); (4) $S_I = 3.75$, $S_G = 3.5$ (low S_I and S_G). The means of the parameters and their standard deviations were calculated for each set of parameters and a given insulin profile. Comparisons were made among four protocols; the lower the SD, the better the precision rendered by an individual protocol.

Results: For each given set of parameters and insulin profile, the means of S_I , S_G , their FSD, and the squared difference between the estimated parameter and its given value are tabulated in Table 6. Each mean value was calculated from 100 experiments generated by the computer. The means from four sets of parameters were summarized for each insulin profile corresponding to its specific protocol (Table 7). The squared difference between estimated parameter and its given value, the standard deviation of the parameter, and FSD for parameter estimation were ranked among the four protocols. The values were designated from the lowest to the highest (best to worst) as 1, 2, 3, 4. The ranks were added up for each protocol; the lower the summed rank,

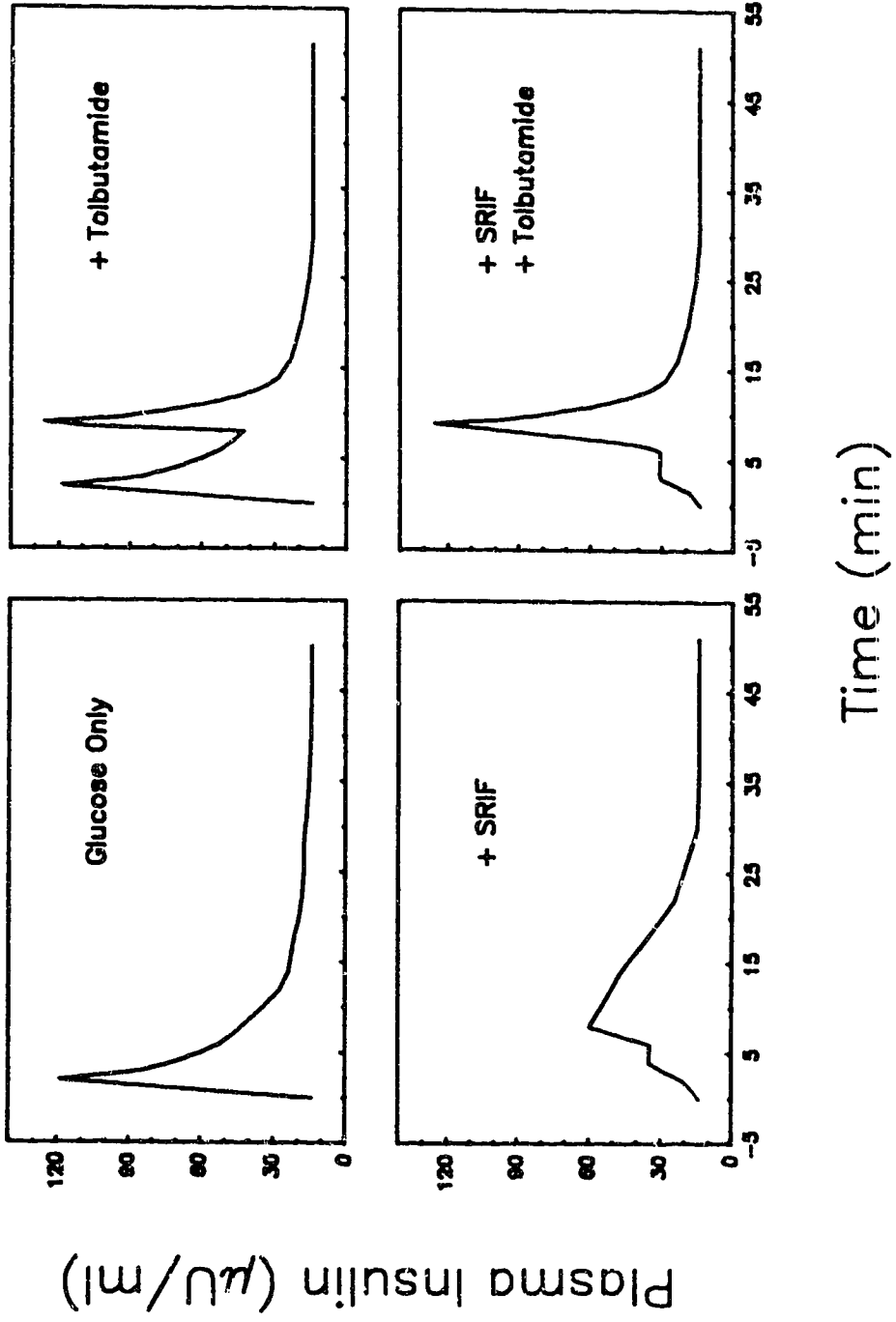


Fig. 9. The four insulin profiles representing the four FSIGT protocols. Upper left, insulin profile of {GLUCOSE} protocol obtained from our experiments; lower left, {SOMATOSTATIN + GLUCOSE} protocol obtained from experiments by a colleague C.J. Longo [143]; upper right, {GLUCOSE + TOLBUTAMIDE} protocol yielded from the combination of the {GLUCOSE} and {SOMATOSTATIN + GLUCOSE + TOLBUTAMIDE} protocols; and lower right, {SOMATOSTATIN + GLUCOSE + TOLBUTAMIDE} protocol obtained from our experiment.

Table 6. Computer simulation

Parameter Set*	Variable	Insulin Profile				
		GLU	SRF	TOL	SGT	
Set 1	MN S_I	7.56	6.35	6.05	6.13	
	$(DIF S_I)^2$	0.00	1.32	2.09	1.89	
	STD	4.40	1.20	1.40	1.60	
	MN FSD	31.50	9.70	7.70	14.50	
	MN S_G	5.52	5.61	5.99	6.72	
	$(DIF S_G)^2$	2.48	2.23	1.24	0.15	
	STD	4.50	1.30	2.40	1.50	
	MN FSD	42.30	7.50	24.00	7.30	
	Set 2	MN S_I	9.79	7.73	7.03	7.26
		$(DIF S_I)^2$	5.24	0.05	0.22	0.06
STD		4.50	1.80	2.40	2.00	
MN FSD		47.60	6.40	19.10	10.20	
MN S_G		2.05	3.23	2.74	3.07	
$(DIF S_G)^2$		2.11	0.07	0.58	0.33	
STD		3.50	1.40	2.70	1.50	
MN FSD		112.50	14.10	79.10	16.60	

(continued)

	MN S_I	6.23	4.01	4.60	4.68
	$(DIF S_I)^2$	6.14	0.07	0.71	0.86
	STD	3.20	1.20	1.60	1.80
Set 3	MN FSD	56.30	31.40	45.90	28.30
	MN S_G	5.00	6.40	5.42	6.74
	$(DIF S_G)^2$	4.42	0.49	2.82	0.13
	STD	3.20	1.50	2.40	1.40
	MN FSD	64.20	6.40	21.40	6.60

	MN S_I	8.21	6.02	4.96	7.29
	$(DIF S_I)^2$	19.85	5.13	1.47	12.56
	STD	6.70	2.70	2.40	4.60
Set 4	MN FSD	63.00	32.10	36.90	26.10
	MN S_G	2.77	3.71	3.17	3.39
	$(DIF S_G)^2$	0.53	0.04	0.11	0.01
	STD	3.80	1.40	2.10	1.20
	MN FSD	86.30	10.90	40.30	15.90

*, Parameter Set: Set 1, $SI=7.5$, $SG=7.1$; Set 2, $SI=7.5$, $SG=3.5$; Set 3, $SI=3.75$, $SG=7.1$; Set 4, $SI=3.75$, $SG=3.5$. MN S_I , mean estimated S_I ; $(DIF S_I)^2$, the sum of squared difference between the computer estimated S_I and the submitted S_I ; STD, the standard deviation of the parameter; MN FSD, the mean fractional standard deviation; MN S_G , mean estimated S_G ; $(DIF S_G)^2$, the squared difference between the computer estimated S_G and the submitted S_G .

Table 7. The summary of computer simulation.

Parameters	Insulin Profiles					
	GLUCOSE (Rank)	SRF (Rank)	TOL (Rank)	SGT (Rank)		
MN S _I	7.95	6.03	5.66	6.34		
(DIF S _I) ²	7.81	1.64	1.12	3.84	3	
STD	4.70	1.73	1.95	2.50	3	
MN FSD	49.60	19.90	27.38	19.78	1	
MN S _G	3.84	4.74	4.33	5.23		
(DIF S _G) ²	2.39	0.71	1.19	0.16	1	
STD	3.75	1.40	1.40	1.40	1.5	
MN FSD	76.33	9.73	11.35	11.60	2	
Sum of Ranks	24	9.5	15			11.5

Parameter Sets: Set 1, S_I=7.5, S_G=7.1; Set 2, S_I=7.5, S_G=3.5; Set 3, S_I=3.75, S_G=7.1; Set 4, S_I=3.75, S_G=3.5. SRF, {SOMATOSTATIN + GLUCOSE}; TOL, {GLUCOSE + TOLBUTAMIDE}; and SGT, {SOMATOSTATIN + GLUCOSE + TOLBUTAMIDE}.

the better the estimation of parameters by the protocol. The {GLUCOSE} protocol had the highest rank; {SRF} and {SGT} protocols appeared to be better than the {TOL} protocol.

Conclusions: The computer simulation study suggested that the additional injection of somatostatin was important to improve the overall estimation of parameters by the minimal model when compared to the original protocol. In the tested protocols the {SRF} and {SGT} protocols were better than the {GLUCOSE} and {TOL} protocols.

Group 5. Insulin dose response / high fat diet study

Hypothesis: Feeding of a high fat diet is proposed to lead to insulin resistance in rats. Insulin dose-response studies should be able to characterize the kinetics of insulin sensitivity (the saturation dose) and determine the optimal insulin dose for the FSIGT protocol. Further increasing the number of samples should augment the parameter estimation.

Methods: Male SD rats were divided into two groups: high fat diet (HFD) and control (CN). The CN animals were fed Wayne Rodent BOLX 8604 ad libitum with 11.5 % of calories as fat (Table 8). A HFD was prepared with 53.5 % fat in calories with P/S ratio of 0.25 (polyunsaturated / saturated fat) in Dr. T. Clandinin's laboratory. The powdered ingredients (proteins, carbohydrates, vitamins, mineral mix, and fiber) were mixed, and the stearin was melted on hot plate and mixed with unsaturated fat (safflower and linseed). The fat mixture was gradually

Table 8. Components of standard chow diet and high-fat-diet

	Chow	High-Fat-Diet

Percent of energy (% kcal)		
Protein	28.5	26.1
Fat	11.5	53.5
Carbohydrate	59.9	20.5

Percent of weight (%)		
Protein	24.5	26.7
Fat	4.4	29.3
Carbohydrate	51.4	23.0

Total energy (kcal/g)	3.43	4.49

added to the powder and well mixed. The animals had either HFD or normal diet for at least three weeks prior to the experiments.

The insulin dose response of FSIGT study was conducted in high fat diet fed SD rats, and in standard chow fed animals as a control group. A total of sixty experiments were conducted on 11 HFD and 11 CN rats. Glucose was given as before and insulin was injected at 9 min at various doses. Five insulin doses were assigned in the thirty experiments of CN rats: 0.01, 0.015, 0.02, 0.025, 0.03 U/kg. In the HFD group, the insulin dose was increased to 0.04 U/kg; seven doses from 0.01 to 0.04 at 0.005 interval were used in thirty FSIGTs.

In an effort to further increase the number of samples, especially the samples for glucose pattern, a sampling device was designed by Dr. Jonathan Tyler for direct blood sampling. Only 25 μ l blood is required for determination of whole blood glucose concentration by a Yellow Springs Instrument Co. (YSI) glucose analyzer. The sampling device, which has a cylindrical plexiglass sampling port with an injectable rubber septum, was connected to the blood sampling catheter, so that the YSI pipette needle can draw blood (25 μ l) through the rubber septum without any blood waste.

The animal was fasted in the plastic shoebox cage with free access to water for 9 hours and transferred to the experimental setting (plexiglass box with holes) half an hour before the experiment. The sampling period was extended to 120 minutes to make sure that the steady-state of glucose was achieved in normal or high-fat-diet fed

animals. A total of 24 samples were taken over the period of 120 min. Twenty-four samples (25 μ l each) were taken to measure blood glucose values directly in the YSI glucose analyzer during the experiment and fourteen blood samples (75 μ l each) were drawn for determination of plasma insulin concentrations. The total blood loss is limited to within 10% of the whole blood volume. The blood sampling for glucose was followed the schedule with additional insulin samples at the underlined times: -6, -2, 1, 2.5, 3.5, 5, 6.5, 9, 10, 11, 12.5, 14, 16, 18, 20, 23, 26, 30, 35, 40, 50, 70, 90, 120 min.

Results: Fig. 10 shows an example of an experiment with 24 data points. The initial insulin peak was stimulated by glucose administration and the second peak of insulin was evoked by insulin injection (in this particular experiment the insulin dose was 0.03 U/kg). The observed glucose and model fit of the glucose kinetics are shown in the bottom panel. The second insulin peak resulted in an undershoot of glucose dynamics and then a return to the basal value. Some animals became infected after several experiments as Coagulase negative Staphylococcus and Serratia marcescens were isolated from the blood cultures.

A portion of the insulin dynamics during the FSIGT are shown in Fig. 11 to illustrate the insulin peak values with different insulin doses. The CN and HFD animals had similar values for both the initial and the second insulin peaks. When the insulin areas above basal were plotted against the insulin doses (Fig. 12), insulin areas from 0 to 8 minute (before the insulin administration) remained unchanged as expected at the various insulin doses, while the 8 to 120 minute insulin areas

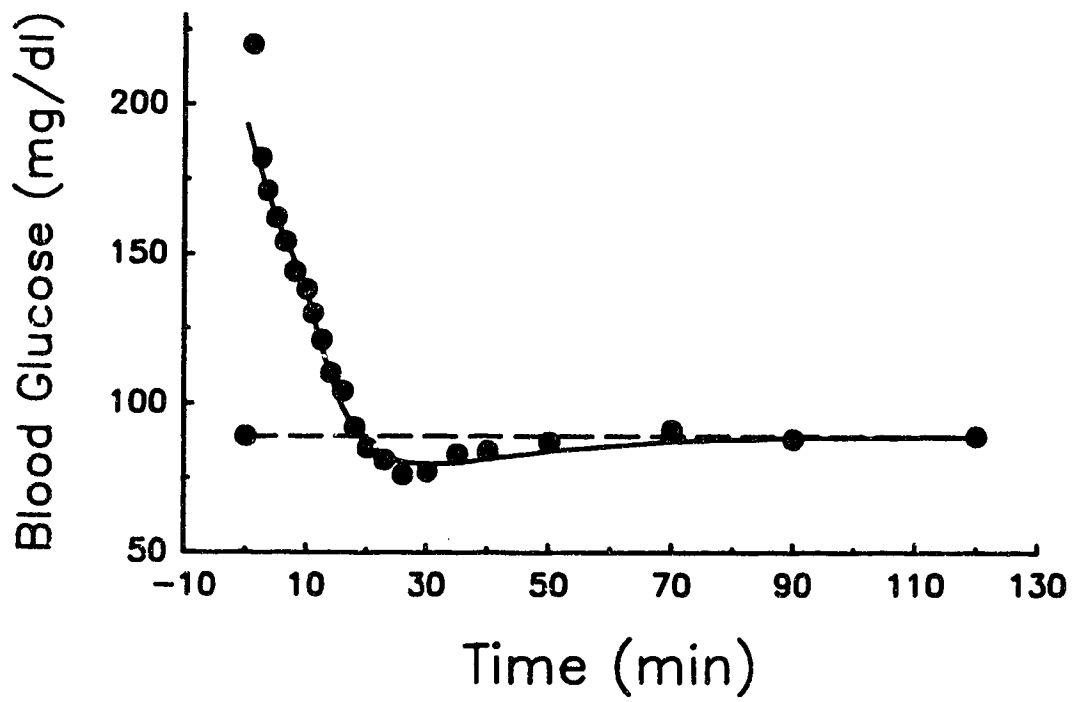
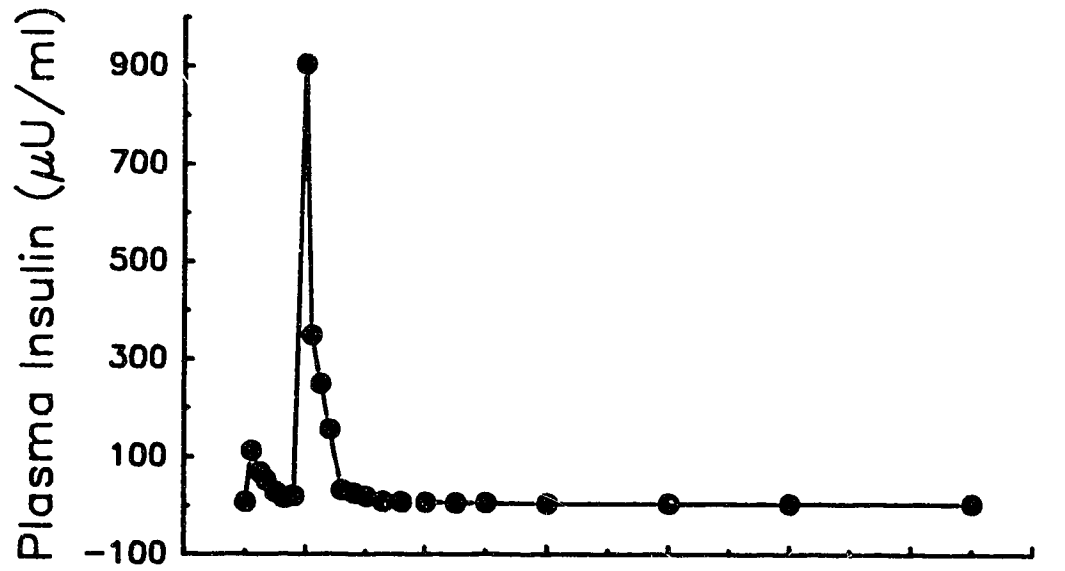


Fig. 10. An experiment of {GLUCOSE + INSULIN} protocol on a control animal in the insulin dose response / high-fat-diet study. The glucose was injected at 0 minute and insulin (0.03 U/kg in this experiment) was given at the 9th minute. The blood glucose was shown in closed circles in the lower panel, and the solid line is the computer generated model fit. The dashed line gives the basal glucose level.

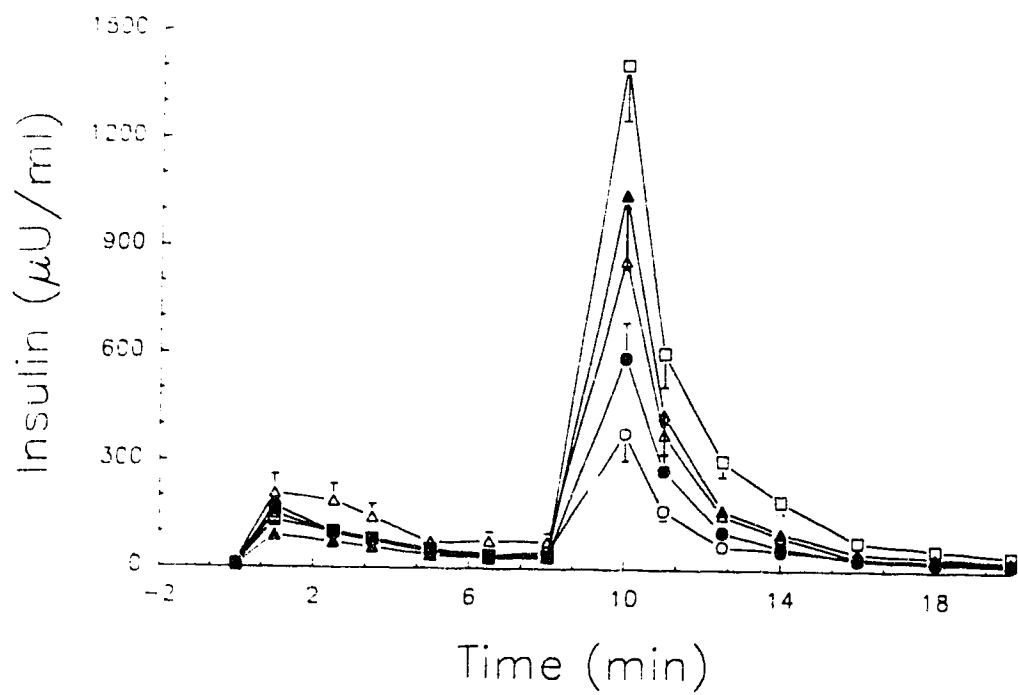
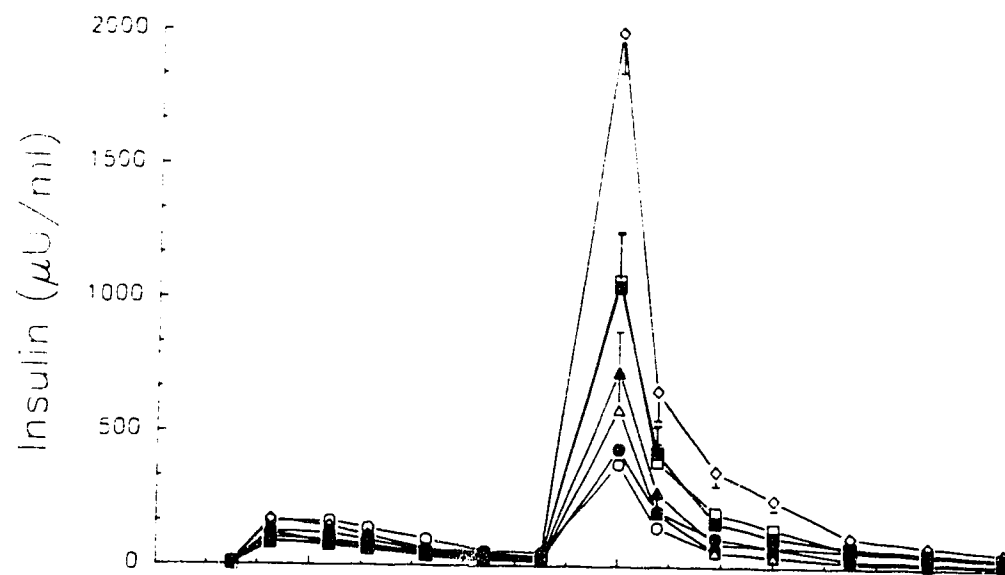


Fig. 11. A section of insulin dynamics (from 0 to 20 minutes) of FSIGT in the insulin dose response / high-fat-diet study. The control group was given in the lower pannel and high-fat-diet group in the upper pannel. The open circles, insulin dose 0.01 U/kg; filled circles, 0.015 U/kg; open triangles, 0.02 U/kg; filled triangles, 0.025 U/kg; open squares, 0.03 U/kg; filled squares, 0.035 U/kg; and open diamonds, 0.04 U/kg.

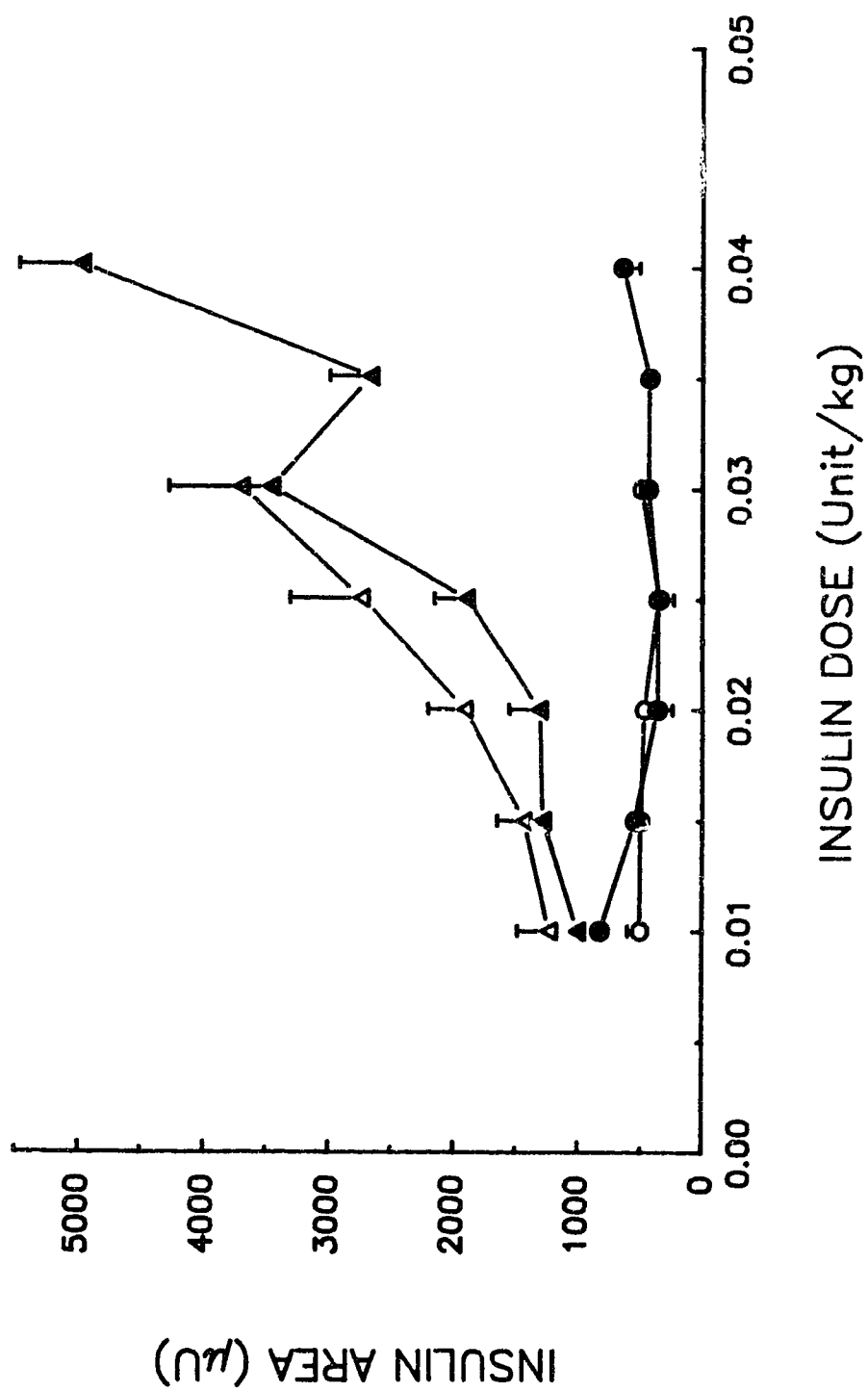


Fig. 12. The insulin areas vs. the insulin doses. The open circles and triangles show the insulin areas from 0 to 8 and 8 to 120 minutes respectively in the control group. The close circles and triangles correspond the insulin areas from 0 to 8 and 8 to 120 minutes respectively in the high-fat-diet groups. No significant difference was given by student t test between the two diet groups.

increased along with the insulin dose. The insulin areas were not significantly different between control and high-fat diet groups for both 0 to 8 minute and 8 to 120 minute periods.

To clarify the effect of different insulin doses on the glucose utilization, the rate of glucose disappearance was plotted vs. time for each of the insulin doses (Fig. 13). The glucose disappearance rate was almost superimposable for CN and HFD groups except that greater variation existed in HFD animals. Additionally, the rate of glucose disappearance was not changed despite the fact that various insulin doses were used at 9 minutes.

Table 9 lists the parameters of the model, and of insulin and glucose kinetics. Two-way analysis of variance was performed using the SAS computer program to determine the individual effect of diet and/or insulin dose on these parameters. No significant difference of the effects of diet or insulin dose was found for S_I and K_G . The S_G estimation appeared to be statistically different between the two groups of diets according to two-way ANOVA. As expected, the overall insulin area and insulin area from 8 to 120 minute were affected by the factor of insulin dose. The parameters were summarized and analyzed for each diet, and no significant difference was observed between these parameters for the two diets (Table 10). Overall, the mean FSDs for S_I and S_G were greatly reduced as compared to previous protocols, and the parameter identifiability of the minimal model was 100 % using the current protocol with 24 data points and 120 minute period.

Fig. 13. The rate of glucose disappearance in the insulin dose response / high-fat-diet study. This glucose disappearance rate was calculated as the change in glucose concentration over the change in time. The bottom pannel shows the control group and the top graph plots the high-fat-diet group. The open circles, insulin dose 0.01 U/kg; filled circles, 0.015 U/kg; open triangles, 0.02 U/kg; filled triangles, 0.025 U/kg; open squares, 0.03 U/kg; filled squares, 0.035 U/kg; and open diamonds, 0.04 U/kg.

Table 9. Rat FSiGT in insulin dose response / high-fat-diet study

Parameters	Diet	
	Chow	HFD
Insulin Dose 0.01 U/kg		
N	6	2
K_G	4.30 ± 0.14	4.85
Total insulin area		
0-8 min	558 ± 111	853
8-120 min	2009 ± 202	1451
S_I	4.74 ± 1.18	3.87
FSD(S_I)	2.07 ± 0.33	2.56
S_G	5.24 ± 0.78	3.70
FSD(S_G)	7.93 ± 0.68	10.53
Insulin Dose 0.015 U/kg		
N	6	1
K_G	4.27 ± 0.47	6.00
Total insulin area		
0-8 min	556 ± 71	580
8-120 min	2337 ± 257	1727
S_I	3.30 ± 0.81	5.72
FSD(S_I)	3.10 ± 0.53	0.57
S_G	6.91 ± 0.70	1.49
FSD(S_G)	6.98 ± 0.81	9.92
Insulin Dose 0.02 U/kg		
N	6	6
K_G	4.15 ± 0.40	3.93 ± 0.30
Total insulin area		
0-8 min	518 ± 150	434 ± 139
8-120 min	2756 ± 320	2279 ± 547
S_I	2.50 ± 0.64	5.55 ± 1.96
FSD(S_I)	3.26 ± 0.74	2.72 ± 0.42
S_G	6.39 ± 0.47	5.04 ± 0.23
FSD(S_G)	6.97 ± 0.67	5.28 ± 0.80

(continued)

Parameters	Diet	
	Chow	HFD
Insulin Dose 0.025 U/kg		
N	6	5
K_G	3.97 ± 0.26	3.86 ± 0.50
Total insulin area		
0-8 min	396 ± 75	398 ± 129
8-120 min	3425 ± 548	2489 ± 352
S_I	1.79 ± 0.18	2.85 ± 0.67
FSD(S_I)	3.04 ± 0.54	4.45 ± 1.19
S_G	6.17 ± 1.36	5.82 ± 0.83
FSD(S_G)	6.04 ± 0.94	4.77 ± 0.47
Insulin Dose 0.03 U/kg		
N	6	6
K_G	4.52 ± 0.37	4.10 ± 0.35
Total insulin area		
0-8 min	546 ± 57	496 ± 58
8-120 min	4455 ± 498	4286 ± 782
S_I	1.67 ± 0.23	2.34 ± 0.42
FSD(S_I)	2.23 ± 0.07	2.21 ± 0.37
S_G	5.35 ± 0.22	4.18 ± 0.60
FSD(S_G)	5.05 ± 0.65	4.92 ± 0.91
Insulin Dose 0.035 U/kg		
N		5
K_G		3.88 ± 0.18
Total insulin area		
0-8 min		475 ± 101
8-120 min		3350 ± 385
S_I		2.71 ± 0.19
FSD(S_I)		3.68 ± 0.81
S_G		7.17 ± 0.90
FSD(S_G)		4.54 ± 0.55

(continued)

Parameters	Diet		
	Chow	HFD	
Insulin Dose 0.04 U/kg			
N		5	
K_G		4.72 ± 0.34	
Total insulin area			
0-8 min		724 ± 150	
8-120 min		6063 ± 428	
S_I		1.35 ± 0.17	
FSD(S_I)		2.29 ± 0.47	
S_G		6.02 ± 1.21	
FSD(S_G)		5.59 ± 1.34	
----- *P values			
	Diet	Dose	Diet x Dose
K_G	0.3225	0.2415	0.3589
Total insulin area			
0-8 min	0.6920	0.2475	0.7233
8-120 min	0.1989	0.0001	0.9658
S_I	0.1250	0.0827	0.4888
FSD(S_I)	0.6722	0.1678	0.3159
S_G	0.0075	0.0895	0.4242
FSD(S_G)	0.4991	0.0035	0.1727

*, P values were calculated by two-way analysis of variance by SAS computer program to test the significance of the diet, insulin dose, and the interaction of the diet and dose. K_G was calculated from 2.5 to 20 minutes of the glucose dynamics. In the insulin dose of 0.01 and 0.015 U/kg, only two and one experiments were performed in the high-fat-diet group. The insulin dose of 0.035 and 0.04 U/kg was only conducted on the high-fat-diet group.

Table 10. Summary of FSIGT experiments in insulin dose response / high-fat-diet study.

Variables	Diets		P [*]
	Control	High-Fat-Diet	
N	30	30	
K _G			
2-8 min	4.18 ± 0.19	3.68 ± 0.17	0.26
2.5-20 min	4.24 ± 0.16	4.21 ± 0.17	0.32
S _I	2.80 ± 0.38	3.17 ± 0.50	0.13
FSD(S _I)	2.74 ± 0.24	2.91 ± 0.33	0.67
S _G	6.01 ± 0.38	5.31 ± 0.40	0.01
FSD(S _G)	6.59 ± 0.38	5.56 ± 0.46	0.50
% Identify	100	100	

*, P values were derived from two-way analysis of variance testing the factor of diet. The Insulin Area >BAS is the insulin area above basal level.

Conclusions: The parameter estimation was significantly improved and the identifiability reached 100 % using the protocol with 24 samples. The insulin sensitivity was not significantly different between diets and insulin doses. The optimal insulin doses for rat FSIGT in control and high fat diet groups cannot be determined since the glucose disappearance rates were not different for various insulin doses. This result suggests that the second insulin peak does not affect the rate of glucose clearance, and without the suppression of the initial insulin response, the elevated glucose was back to the basal level before the expression of the action of exogenous insulin. Therefore, the estimation of insulin sensitivity based on the second insulin peak may not be appropriate. The {GLUCOSE + INSULIN} or {GLUCOSE + TOLBUTAMIDE} protocol are not adequate for the rat minimal model/FSIGT. Somatostatin must be used to inhibit the initial insulin response so that the effects of insulin and glucose on glucose disappearance can be differentiated.

DISCUSSION

1. Summary

The minimal model / FSIGT method has already been applied and validated to quantify insulin sensitivity *in vivo* in humans and dogs. This study initiated the adaptation of this model-based approach to the assessment of insulin sensitivity in the rat. Initial studies demonstrated the feasibility of performing an FSIGT in conscious unrestrained rats. With the chronic cannulation of the jugular vein and inferior vena cava, the FSIGT experiment, including intravenous administration of agent(s) and frequent blood sampling, could be performed in rats. Our pilot study in Long Evans rats suggested that the model parameters could be estimated from the FSIGT protocol with only 7 to 8 blood samples, but the percentage of the experiments with identified parameters was low and the fractional standard deviations were high. Injections of somatostatin and tolbutamide were introduced to the FSIGT protocol to alter the insulin dynamics, so that the effects of glucose and insulin on the glucose dynamics could be differentiated.

In comparison to the {GLUCOSE} protocol, the modified {SOMATOSTATIN + GLUCOSE + TOLBUTAMIDE} protocol resulted in a significant improvement in the parameter identifiability and fractional standard deviations. The computer simulation study revealed that the {SOMATOSTATIN + GLUCOSE} and {SOMATOSTATIN + GLUCOSE + TOLBUTAMIDE} protocols resulted in a more accurate and precise parameter estimation than the {GLUCOSE + TOLBUTAMIDE} and {GLUCOSE} protocols. The FSIGT simulation showed that

the protocols with somatostatin resulted in overall better characterization of the parameters. Furthermore, in the high-fat-diet study, without the use of somatostatin, the glucose dynamics remained relatively constant regardless of the amount of the insulin injected, thus the second insulin peak did not have any effect on the glucose dynamics. It appears that somatostatin should be used to suppress the initial insulin response in order to facilitate the model's ability to differentiate the glucose effectiveness and the insulin action. Our experimental results and computer simulation indicate that the {SOMATOSTATIN + GLUCOSE + TOLBUTAMIDE} protocol is the optimal protocol for estimation of insulin sensitivity and glucose effectiveness in the rat.

2. Adaptation of Minimal Model / FSIGT to rat

The minimal model of glucose kinetics was developed and validated in dogs and humans under a variety of normal and pathophysiological conditions. Adaptation of this approach to the rat required consideration of the blood volume available for sampling and the difference of glucose and insulin kinetics between dogs and rats. The optimal protocol and sampling schedule which could accurately characterize the glucose and insulin dynamics are constrained by these factors.

The greatest impediment to accurately describe the dynamic change of glucose and insulin is the limited blood volume of the rat as compared to dogs or humans. If acute losses of approximately 10 % of the total

blood volume are exceeded, the adrenal medulla and sympathetic nerve endings could release sympathetic amines which would result in an increase of the heart rate, constriction of arteriolar beds in muscle and skin, constriction of veins and venous reservoirs, and insulin resistance [139]. The total blood volume of rat is about 6.5 % of the body weight [139]. Previous reports suggested that removal of 5-11 % of total blood volume at a rate of 1 ml/7.5 minutes resulted in no change in plasma corticosterone [139]. It was assumed that a safe sampling volume is 10 % of the total blood volume, which was overestimated to be 10 % of the animal's body weight [139]. McGill et. al. tentatively recommended that investigators limit blood sampling to 15 percent of total blood volume for a single sample and provide special justification for taking volumes greater than 15 percent [139]. However, in our rat FSIGT study, the total blood loss was spread throughout the experiment, and the volume of blood lost was immediately replaced by saline. The total blood loss was less than or equal to the 10 % of the whole blood volume, estimated as 6.5 % of the animal's body weight. For example, the blood taken for a single experiment was less than or equal to 1.95 ml for a typical 300 gram rat.

During an FSIGT, the injection of glucose into normal, conscious dogs resulted in a variety of temporal responses of plasma insulin and glucose; this variation was observed not only between animals but between experiments in the same animal [140]. However, despite wide variation, the insulin response after glucose injection can generally be described as a biphasic pattern with an early peak and a prominent second phase [119, 140]. The insulin levels returned to basal at 70

minute after glucose injection [122]. The insulin action on glucose disappearance was delayed for about 10 minutes with respect to the plasma insulin response [122]. In our rat experiments, the insulin response after glucose injection was a single peak which declined to basal levels by 10 - 12 minutes. The insulin action reached its peak range from 5 to 8 minutes in the rat FSIGT experiments while the plasma insulin peak was detected at 2 min. This suggests that in the rat FSIGT the insulin action was delayed for about 4 minutes with respect to the plasma insulin concentration. The dynamic pattern of glucose is an early exponential fall followed by an undershoot, and then a climb back to basal level in insulin sensitive dogs and rats. In an insulin insensitive animal there is no undershoot during the FSIGT. These glucose dynamic changes are much more rapid in rats than in dogs or humans. The glucose normalized its basal concentration by 15 minutes in rat and between 30 and 60 minutes in normal dogs after the glucose injection.

3. The Number of Blood Samples

As the dynamic change of glucose and insulin is a rather rapid process in the rat compared to that in dog, blood samples should be taken more frequently in order to precisely and accurately define the glucose and insulin dynamics in the rat FSIGT. However, without the apparent disturbance of the animal's physiological state, only limited volume of blood was allowed to be taken for individual experiments.

Though the model was able to estimate the parameters with the protocol using only 7 or 8 blood samples, the identifiability and the fractional standard deviation of the parameters were very poor by the (GLUCOSE) only protocol. From the pilot FSIGT study in Long Evans rats, the timing of insulin peak and of normalization of stimulated insulin was relatively consistent. In the analysis of an FSIGT experiment by the MINMOD computer program, insulin is considered an input variable and glucose is an output variable. The magnitude of insulin dynamics (the basal levels and peak values of insulin, and the time of insulin return to basal) is more important than the description of the moment to moment changes in concentration. The model uses the insulin and a guessed set of parameters as input, solves the equations, and generates a glucose curve. This model-fit is compared to the observed glucose dynamics and a new set of parameters are determined until the best model-fit is achieved. Thus characterization of the moment-to-moment changes in the glucose concentration is important to obtaining the best model-fit and model parameters.

In our original studies we drew 250 μ l of blood to allow for duplicate determination of plasma glucose and plasma insulin concentrations. Since the insulin radioimmunoassay (RIA) provides a sensitive method for measuring insulin concentrations, we decided to draw only enough blood of a single determination of plasma insulin. Also in an effort to increase the numbers of samples without more blood loss, the plasma for insulin RIA was diluted such that less plasma could be taken. 75 μ l of blood is required for insulin RIA, whereas only 10 μ l plasma is needed with the Beckman Glucose Analyzer 2, or 25 μ l blood

is necessary by the YSI Glucose Analyzer for determination of glucose concentration. Thus for each insulin sample we could draw 3 or 4 glucose samples. By not doing duplicate assay of insulin both the glucose and insulin samples could be increased, and the glucose samples could be further increased by giving up a few insulin determinations for extra glucose samples. Providing that the magnitude of insulin dynamics was well defined, it should not significantly affect the parameter estimation with fewer insulin samples than glucose samples in the protocol.

Glucose concentration can be determined from 25 μ l whole blood in the YSI glucose analyzer. With a sampling device placed in the blood sampling line, we were able to have direct access for blood sampling using the YSI analyzer pipette without any blood waste during sample processing. As the minimal model of glucose dynamics counts on the change of the rate of glucose disappearance rather than the absolute value of the glucose concentration, it is reasonable to use the dynamics of whole blood glucose instead of plasma glucose in the model. With the sampling device, we were able to take 24 glucose samples and 14 samples for insulin in a single FSIGT experiment.

When the number of blood samples was increased for better characterization of glucose and insulin dynamics, the insulin action and other model parameters could be more accurately and precisely estimated. In the preliminary FSIGT study where 7 or 8 samples were taken for glucose and insulin, the percentage of experiments with identified parameters was 50 %. As the number of samples increased to fourteen or

seventeen, the ability of the model to identify parameters was enhanced (89%). Having 24 glucose and 14 insulin samples in the rat FSIGT experiments, the identifiability reached 100 % and the fractional standard deviations were markedly reduced.

4. High Fat Diet

In the insulin dose response / high-fat-diet study, the rates of glucose disappearance were not different between the control and high-fat-diet animals, and the insulin response to the glucose load (calculated as the insulin area between 0 to 8 minutes) were also not different between groups. This indicated that the high-fat-diet did not have an effect on the glucose tolerance. Our results were different to previous reports where a high-fat-diet was documented to induce impaired glucose metabolism and insulin action [20, 21, 129]. One difference to account for this discrepancy may be in the age of the animal at the commencement of the diet. The animal age at which the high-fat-diet feeding was started was on weaning or within one month of birth in most of the reports, whereas the start age for the diet in our study was a month after weaning or 7 to 8 weeks of age. The diet which was stated to lead to insulin resistance had 67 or 70 % of the energy as fat [124, 126, 133, 136]. In one report, a diet in which fat composed 50 % of the calories, with feeding beginning at the age of weaning, led to impaired glucose tolerance [135]. In our insulin dose response / high-fat-diet study, the animals were fed a diet with 53.5 % energy as fat, but this may have been too low because of the age at which the diet was initiated.

Another factor which may account for our not obtaining a difference in insulin action between high fat and chow fed rats was the presence of sepsis. Whole body insulin resistance has been demonstrated in septic patients [149, 150]. At three month after sepsis, the insulin sensitivity was not fully recovered [150]. Lang et. al. reported that infection caused a decreased rate of insulin-mediated glucose uptake (IMGU) [151] and an increase in the NIMGU (noninsulin-mediated glucose uptake) [152] in rats. Sepsis increased the rate of glucose disappearance in nondiabetic rats but had no effect in diabetic animals [153]. In the diabetic rats infection did not further worsen the insulin resistance [153, 154], while in nondiabetic animals sepsis produced peripheral insulin resistance [154]. In our study of insulin dose response / high fat diet, there was evidence of sepsis in both control and high-fat-diet rats. Sepsis may further complicate the effect of a high-fat-diet on glucose tolerance and insulin sensitivity.

5. Insulin Dose Response Study

The {GLUCOSE + INSULIN} protocol was performed in control and high-fat-diet fed animals using various insulin doses. The insulin sensitivity index was poorly distinct despite that varying insulin doses were used. With the {GLUCOSE + INSULIN} protocol, the rates of glucose clearance were unaffected by the different insulin boluses given. It appears that the injected insulin did not influence the glucose disappearance rate. Without the suppression of the initial insulin response by somatostatin, the first insulin peak accelerated the rate of

glucose disposal; and the glucose concentration declined to the basal level before the expression of insulin action from the injected insulin. The S_G estimation might contain the effect of elevated insulin, and the model parameters S_I and S_G might not be fully differentiated. Given the similar rate of glucose clearance and insulin sensitivity between diet groups, the glucose effectiveness was lower in high-fat-diet animals than that in control group. The results suggest that the use of somatostatin is essential for the model to differentiate the S_I and S_G in the rat FSIGT protocol.

6. Computer Simulation

Simulation is a process of calculating the response of a model by substituting values for its parameters, and a range of values of the independent variables. Thus it is possible to investigate the characteristics of the model under a variety of conditions. Testing the responses of a model provides an understanding of its potential, and it can be used to study the effects of experimental uncertainty on the characteristics of a model [141].

"Monte Carlo" simulation is used to investigate the statistical properties only of the model equations, rather than their ability to describe the real system [141]. Monte Carlo simulation cannot prove whether or not a model is "true". The behavior of the real system can be only studied by experimentation. Monte Carlo simulation was employed to assess the possible protocols in the rat FSIGT. Parameter values, estimated from the initial experiment, were used to simulate or

artificially generate output from the model equations. Appropriate errors were added to the output to resemble the measurement uncertainties of the experiment. The model was then fitted to the simulated data and new parameter estimates were made. This process was repeated to generate a series of parameter estimates from which a mean and standard deviation could be calculated. The parameters were then compared with the estimates from the simulation to determine whether the original parameter uncertainties were plausible. Therefore, simulation was used to gain information about the way in which the model would behave under varying conditions, and its response to the magnitude and distribution of measurement uncertainty. In the current study, simulation was applied to test four different FSIGT protocols .

The {GLUCOSE}, {SOMATOSTATIN + GLUCOSE}, {GLUCOSE + TOLBUTAMIDE}, and {SOMATOSTATIN + GLUCOSE + TOLBUTAMIDE} protocols which result in four distinct insulin dynamics were examined by computer simulation. When the overall precision, accuracy and identifiability of the parameter estimation were compared among the four protocols, the {SOMATOSTATIN + GLUCOSE} and {SOMATOSTATIN + GLUCOSE + TOLBUTAMIDE} protocols appeared to be better than the {GLUCOSE} and {GLUCOSE + TOLBUTAMIDE} protocols. This suggested that somatostatin is necessary in the rat FSIGT protocol.

7. The Role of Somatostatin and Tolbutamide in Rat FSIGT

Somatostatin (SRIF) is a peptide hormone distributed widely in the body. In rats the highest concentrations of SRIF have been found in isolated pancreatic islets and in the pituitary stalk median eminence

region [142]. The most dominant function of SRIF is to inhibit the release of peptide or amine hormones in three areas: hypothalamus-hypophysis, stomach and small intestine, and pancreas. In the endocrine pancreas somatostatin inhibits the secretion of insulin and glucagon. In the exocrine pancreas SRIF suppresses bicarbonate, water, and pancreatic enzymes. Pathophysiologically, the somatostatin content of the pancreas and the number of somatostatin-secreting D cell appears to be increased in type I diabetes mellitus in man and alloxan diabetes in animals [142].

In dogs the FSIGT protocol has been modified by somatostatin injection at 1 minute prior to glucose load or tolbutamide at 20 minutes post glucose injection [119]. The computer simulation demonstrated that with the tolbutamide or somatostatin protocols the variability of S_G estimates was reduced and FSDs for the parameter estimates were decreased [119]. The TOLB protocol has been used as a standard FSIGT protocol in humans and dogs. Tolbutamide injection rapidly induced a second insulin peak which was about equal to the first peak, while the insulin secretion during first 19 minutes was not different between GLUCOSE and TOLB protocols [119]. With the SRIF protocol, the insulin response was delayed and increased gradually whereas the total insulin secretion was not statistically below that of the GLUCOSE protocol in normal dogs [119].

As somatostatin or tolbutamide has been used in the dog FSIGTs to improve the quantification of model parameters, the rat FSIGT protocol was modified by the addition of somatostatin. Data collected by others

suggests that a protocol of {SOMATOSTATIN + GLUCOSE} led to an inadequate insulin response resulting from the suppression of insulin release by somatostatin [143]. Thus insulin secretagogues or insulin may be necessary to induce a sufficient insulin peak. In the modified rat FSIGT protocol, {SOMATOSTATIN + GLUCOSE + TOLBUTAMIDE}, somatostatin was given -0.5 minute before glucose and tolbutamide were injected at 8 minutes post glucose (at about the middle of the glucose decline). Our experimental results suggested that the ability of the model to identify and quantify parameters was significantly enhanced in the {SOMATOSTATIN + GLUCOSE + TOLBUTAMIDE} protocol as compared to the {GLUCOSE} protocol. The FSD for S_I and S_G was reduced from 27.3 ± 4.4 and 27.0 ± 4.0 in {GLUCOSE} to 6.7 ± 0.6 and 10.1 ± 2.5 percent in the modified protocol ($P < 0.0001$ and $P = 0.015$ respectively). Thus, the experiments have demonstrated that the {SOMATOSTATIN + GLUCOSE + TOLBUTAMIDE} protocol results in a significant improvement of the parameter estimation.

In the rat FSIGT, the physiological disturbance of glucose homeostasis induced by glucose injection only lasted about 15 minutes. During the rapid dynamics of glucose and insulin, it is difficult for the minimal model to distinguish insulin action and glucose effectiveness from the {GLUCOSE} protocol. With the limitation of blood loss and time for sampling, the subtle changes in the rate of glucose disappearance may not have been precisely characterized. The injection of somatostatin suppressed the initial insulin response, so that the early phase of glucose disappearance was attributed to glucose itself without the action of additional insulin (glucose effectiveness) and the delayed insulin appearance in the plasma accelerated the glucose

clearance (insulin sensitivity). Therefore, the addition of somatostatin to the rat FSIGT protocol could facilitate differentiation between the effects of glucose and insulin on the rate of glucose disappearance.

In the group 3 study where the {GLUCOSE} and {SOMATOSTATIN + GLUCOSE + TOLBUTAMIDE} protocols were directly compared, the S_G estimation was statistically lower in the modified protocol than that in {GLUCOSE} protocol, whereas the S_I estimation was not different in the two protocols. The better parameter estimation from the {SOMATOSTATIN + GLUCOSE + TOLBUTAMIDE} protocol were evidenced by the lower FSD. The estimation of S_G in the {GLUCOSE} protocol might be contaminated with the effect of insulin since the initial insulin peak was not inhibited, while in the modified protocol the somatostatin augmented the model's ability to differentiate between S_G and S_I .

Though the use of SRIF was necessary in the rat FSIGT experiment, the effect of somatostatin on insulin action is controversial in the literature. Continuous infusion of somatostatin (200 $\mu\text{g/h}$ for 2 hours) during hyperinsulinemic-euglycemic clamping was reported to potentiate insulin-stimulated glucose uptake in normal individuals but not in NIDDM subjects [144]. During normal insulinemia clamp, somatostatin infusion (0.8 $\mu\text{g/kg/min}$ for 150 min) resulted in an increase in glucose clearance in dogs [145]. However, others reported that infusion of somatostatin (0.8 $\mu\text{g/kg/min}$ for 3 hours) during a hyperinsulinemic-euglycemic clamp did not have an effect on epinephrine-stimulated glucose production in dogs [147], and somatostatin infused at 250 $\mu\text{g/h}$ for 3 hours did not

alter insulin-mediated glucose disposal in normal subjects [148]. Baron et. al. demonstrated that somatostatin infused at a higher dose (600 $\mu\text{g}/\text{h}$ for 3 hours) did not increase glucose disposal in humans [146].

In our rat FSIGT experiments somatostatin was used as a single injection of 16 $\mu\text{g}/\text{kg}$, and the administered dose was much lower than these used in previous reports of SRIF effects on insulin action (e.g., 0.8 $\mu\text{g}/\text{kg}/\text{min}$ for 3 hour equal to 144 $\mu\text{g}/\text{kg}$). Also the previous reports were documented in humans and dogs, and the effect of somatostatin in rat should be further investigated. Thus, at this much lower dose being used, the injection of somatostatin appeared not likely to have an effect on insulin action in rat FSIGT.

8. Conclusions

The current studies suggest that the minimal model / frequently sampled intravenous glucose tolerance test can be applied to the rat to estimate insulin sensitivity. The ability of the model to quantify the parameters can be markedly improved by increasing the number of blood samples to measure glucose and insulin concentrations. Somatostatin must be added to the protocol to achieve a more precise, accurate estimation of parameters and a higher identifiability. The {SOMATOSTATIN + GLUCOSE + TOLBUTAMIDE} protocol is the optimal protocol for rat FSIGTs. Further validation of the rat FSIGT protocol requires direct comparison of glucose clamp and minimal model / FSIGT techniques.

REFERENCES

1. Seifter S., and S. Englard. Carbohydrate metabolism. In: Diabetes mellitus. Ed., M. Ellenberg and H. Rifkin. Med. Exam. Publishing Co. Inc. pp1-46, 1983.
2. Felig P. Physiological action of insulin. In: Diabetes Mellitus. Ed., M. Ellenberg and H. Rifkin. Med. Exam. Publishing Co. Inc. pp77-88, 1983.
3. Baron A.D., G. Brechtel, P. Wallace, and S.V. Edelman. Rates and tissue sites of non-insulin- and insulin mediated glucose uptake in humans. Am. J. Physiol. 255:E769-74, 1988.
4. Bondy P.K., W.L. Bloom, V.S. Whitner, and B.W. Farrar. Studies of the role of the liver in human carbohydrate metabolism by the venous catheter technic. II. Patients with diabetic ketosis, before and after the administration of insulin. J. Clin. Invest. 28:1126-33, 1949.
5. Kahn B.B., and S.W. Cushman. Subcellular translocation of glucose transporters: role in insulin action and its perturbation in altered metabolic states. Diabetes Metab. Rev. 1:203-27, 1985.
6. Rizza R.A., L.J. Mandarino, and J.E. Gerich. Dose-response characteristics for effects of insulin on production and utilization of glucose in man. Am. J. Physiol. 240:E630-39, 1981.
7. Best J.D., G.J. Jr Taborsky, J.B. Halter, and D. Jr Porte. Glucose disposal is not proportional to plasma glucose level in man. Diabetes 30:847-50, 1981.
8. Gottesman I., L. Mandarino, C. Verdonk, R. Rizza, and J. Gerich. Insulin increases the maximum velocity for glucose uptake without

- altering the Michaelis Constant in man. *J. Clin. Invest.* 70:1310-14, 1982.
9. Felig P., J. Wahren, and Hendler. Influence of maturity-onset diabetes on splanchnic glucose balance after oral glucose ingestion. *Diabetes* 27:121-26, 1978.
 10. Orci L. The cell biology of proinsulin processing. In: Pathogenesis of non-insulin dependent diabetes mellitus. Ed., V. Grill and S. Efendic. Reaven Press, pp1-26, 1988.
 11. Malaisse W.J. Insulin release: physiology and pathophysiology of nutrient metabolism in pancreatic islet cells. In: Pathogenesis of non-insulin dependent diabetes mellitus. Ed., V. Grill and S. Efendic. Reaven Press, pp27-38, 1988.
 12. Gold G. Insulin structure and biosynthesis. In: Insulin secretion. Ed., B. Draznin, S. Melmed, and D. LeRoith. Alan R. Liss, Inc. pp25-35, 1989.
 13. Draznin B., and R. Dahl. Cell biology of insulin secretion. In: Insulin secretion. Ed., B. Draznin, S. Melmed, and D. LeRoith. Alan R. Liss, Inc. pp37-47, 1989.
 14. Kasanicki M.A. and P.F. Pilch. Regulation of glucose-transporter function. *Diabetes Care* 13:219-27, 1990.
 15. Saltiel A.R. Second messengers of insulin action. *Diabetes Care* 13:244-56.
 16. Rosen O.M. Structure and function of insulin receptor. *Diabetes* 38:1508-11, 1989.
 17. Bell G.I., T. Kayano, J.B. Buse, C.F. Burant, J. Takeda, D. Lin, H. Fukumoto, and S Seino. Molecular biology of mammalian glucose transporters. *Diabetes Care* 13:198-208, 1990.

18. Klip A., and M.R. Paquet. Glucose transport and glucose transporters in muscle and their metabolic regulation. *Diabetes Care* 13:228-43, 1990.
19. Carpentier J.L. The cell biology of the insulin receptor. *Diabetologia* 32:627-35, 1989.
20. Storlien L.H., D.E. James, K.M. Burleigh, D.J. Chisholm, and E.W. Kraegen. Fat feeding causes widespread in vivo insulin resistance, decreased energy expenditure, and obesity in rats. *Am. J. Physiol.* 251:E576-83, 1986.
21. Kraegen E.W., D.E. James, L.H. Storlien, K.M. Burleigh, and D.J. Chisholm. In vivo insulin resistance in individual peripheral tissues of the high fat fed rat: assessment by euglycemic clamp plus deoxyglucose administration. *Diabetologia* 29:192-98, 1986.
22. Allsop J.R., R.R. Wolfe, and J.F. Burke. Glucose kinetics and the responsiveness to insulin in the rat injured by burn. *Surg. Gynecol. Obstet.* 147:565-73, 1978.
23. Turinsky J., T.M. Saba, W.A. Scoville, and T. Chesnut. Dynamics of insulin secretion and resistance after burns. *J. Trauma* 17:344-50, 1977.
24. Ferrannini E., G. Buzzigoli, R. Bonadonna, M.A. Giorico, M. Oleggini, L. Graziade, R. Pedrinel, L. Brandi, and S. Bevilacq. Insulin resistance in essential hypertension. *N. Engl. J. Med.* 317:350-57, 1987.
25. Olefsky J.M. Insulin antagonists and resistance. In: *Diabetes mellitus*. Ed., M. Ellenberg and H. Rifkin. Med. Exam. Publishing Co. Inc. pp151-178, 1983.

26. Rosen O.M., R. Herrera, Y. Olowe, L.M. Petruzzelli, and M.H. Cobb. Phosphorylation activates the insulin receptor tyrosine protein kinase. *Proc. Natl. Acad. Sci. USA* 80:3237-40, 1983.
27. Kolterman O.G., J. Insel, M. Saekow, and J.M. Olefsky. Mechanisms of insulin resistance in human obesity: evidence for receptor and post-receptor defects. *J. Clin. Invest.* 68:957-69, 1980.
28. Ciaraldi T.P., O.G. Kolterman, and J.M. Olefsky. Mechanisms of the postreceptor defect in insulin action in human obesity: decrease in intrinsic activity of the glucose transport system. *J. Clin. Invest.* 68:875-80, 1981.
29. Kashiwagi A., C. Bogardus, S. Lillioja, T.P. Hueckste, D. Brady, M.A. Verso, and J.E. Foley. In vitro insensitivity of glucose transport and antilipolysis to insulin due to receptor and postreceptor abnormalities in obese Pima Indians with normal glucose tolerance. *Metabolism* 33:772-77, 1984.
30. Garvey W.T. Cellular and molecular pathogenesis of insulin resistance. In: *Insulin action*. Ed., B. Draznin, S. Melmed, and D. LeRoith. Alan R. Liss, Inc. pp79-95, 1989.
31. Hollenbeck C.B., Y-D I. Chen, and G.M. Reaven. A comparison of the relative effects of obesity and non-insulin-dependent diabetes mellitus on in vivo insulin-stimulated glucose utilization. *Diabetes* 33:622-26, 1984.
32. Kolterman O.G., R.S. Gray, J. Griffin. Receptor and post-receptor defects contribute to the insulin resistance in non-insulin dependent diabetes mellitus. *J. Clin. Invest.* 68:957-69, 1981.
33. Himsworth H.P. Diabetes mellitus. Its differentiation into insulin-sensitive and insulin insensitive types. *Lancet* 230:127-30, 1936.

34. Himsworth H.P., and R.B. Kerr. Insulin-sensitive and insulin-insensitive types of diabetes mellitus. *Clin. Sci.* 4:119-52, 1939.
35. Himsworth H.P. The syndrome of diabetes mellitus and its causes. *Lancet* 256:465-72, 1949.
36. Himsworth H.P., and R.B. Kerr. Age and insulin sensitivity. *Clin. Sci.* 4:153-57, 1939.
37. Yalow R.S., and S.A. Berson. Immunoassay of endogenous plasma insulin in man. *J. Clin. Invest.* 39:1157-75, 1960.
38. Reaven G., and R. Miller. Study of the relationship between glucose and insulin responses to an oral glucose load in man. *Diabetes* 17:560-69, 1968.
39. Reaven G., J. Moore, and M. Greenfield. Quantification of insulin secretion and *in vivo* insulin action in non-obese and moderately obese individuals with normal glucose-tolerance. *Diabetes* 32:600-604, 1983.
40. Karam J.H., G.M. Grodsky, and P.H. Forsham. Excessive insulin response to glucose in obese subjects as measured by immunochemical assay. *Diabetes* 12:197-204, 1963.
41. Yalow R.S., S.M. Glick, J. Roth, and S.A. Berson. Plasma insulin and growth hormone levels in obesity and diabetes. *Ann. NY Acad. Sci.* 131:357-73, 1965.
42. Soerjodibroto W.S., C.R.C. Heard, and A.N. Exton-Smith. Glucose tolerance, plasma insulin levels, and insulin sensitivity in elderly patients. *Aging* 8:65-74, 1979.
43. Reaven E., D. Wright, C.E. Mondon, R. Solomon, H. Ho, and G.M. Reaven. Effect of age and diet on insulin secretion and insulin action in the rat. *Diabetes* 32:175-80, 1983.

44. Hollingsworth D.R. Alterations of maternal metabolism in normal and diabetic pregnancies: difference in insulin-dependent, non-insulin-dependent, and gestational diabetes. *Am. J. Obstet. Gynecol.* 146:417-29, 1983.
45. Fisher P.M., H.W. Sutherland, and P.D. Bewsher. The insulin response to glucose infusion in gestational diabetes. *Diabetologia* 19:10-14, 1980.
46. Bergman R.N., D.T. Finegood, and M. Ader. Assessment of insulin sensitivity in vivo. *Endocrine Reviews* 6:45-86, 1985.
47. Shen W.W., G.M. Reaven, and J.W. Farquhar. Comparison of impedance to insulin mediated glucose uptake in normal and diabetic subjects. *J. Clin. Invest.* 49:2151-60, 1970.
48. Olefsky J., J.W. Farquhar, and G.M. Reaven. Relationship between fasting plasma insulin level and resistance to insulin mediated glucose uptake in normal and diabetic subjects. *Diabetes* 22:507-13, 1973.
49. Joost H.G., and T.M. Weber. The regulation of glucose transport in insulin-sensitive cells. *Diabetologia* 32:831-38, 1989.
50. Reaven G.M., R. Bernstein, B. Davis, and J.M. Olefsky. Nonketotic diabetes mellitus: insulin deficiency or insulin resistance. *Am. J. Med.* 60:80-88, 1976.
51. Ginsberg H., G. Kimmerling, J.M. Olefsky, and G.M. Reaven. Demonstration of insulin resistance in untreated adult onset diabetic subjects with fasting hyperglycemia. *J. Clin. Invest.* 55:454-61, 1975.

52. Ginsberg H., J.M. Olefsky, and G.M. Reaven. Further evidence that insulin resistance exists in the patients with chemical diabetes. *Diabetes* 23:674-78, 1974.
53. Asayama K., S. Amemiya, K. Kato, and M. Shimizu. In vivo insulin sensitivity and insulin binding to erythrocytes in children: insulin resistance in obese children. *Endocrinol. Jpn.* 29:575-81, 1982.
54. Nagulesparan M., P.J. Savage, R.H. Unger, and P.H. Bennett. A simplified method using somatostatin to assess in vivo insulin resistance over a range of obesity. *Diabetes* 28:980-83, 1979.
55. Gingsberg H.N. Investigation of insulin resistance during diabetic ketoacidosis: role of counter-regulatory substances and effect of insulin therapy. *Metabolism* 26:1135-46, 1977.
56. Gingsberg H.N. Investigation of insulin sensitivity in treated subjects with ketosis-prone diabetes mellitus. *Diabetes* 26:278-83, 1977.
57. Reaven G.M., W.S. Sageman, and R.S. Swenson. Development of insulin resistance in normal dogs following alloxan-induced insulin deficiency. *Diabetologia* 131:459-62, 1977.
58. Dallaglio E., F. Chang, H. Chang, D. Wright, and G.M. Reaven. Effect of exercise training and sucrose feeding on insulin-stimulated glucose uptake in rats with streptozotocine-induced deficient diabetes. *Diabetes* 32:165-68, 1983.
59. Reaven G.M., M.S. Greenfield, C.E. Mondon, M. Rosenthal, D. Wright, and E.P. Reaven. Dose insulin removal rate from plasma decline with age? *Diabetes* 31:670-73, 1982.

60. Kolterman O.G., G.M. Reaven, and J.M. Olefsky. Relationship between in vivo insulin resistance and decreased insulin receptors in obese man. *J. Clin. Endocrinol. Metab.* 48:487-94, 1979.
61. Andres R., R. Swerdloff, T. Pozefsky, and D. Coleman. Manual feedback technique for the control of blood glucose concentration. In: *Automation in Analytical Chemistry*. Ed., L.T. Skeggs, Jr. New York:Mediad, pp486-91, 1966.
62. Sherwin R.S., K.J. Kramer, J.D. Tobin, P.A. Insel, J.E. Liljenquist, M. Berman; and R. Andres. A model of the kinetics of insulin in man. *J. Clin. Invest.* 53:1481-92, 1974.
63. Insel P.A., J.E. Liljenquist, J.D. Tobin, R.S. Sherwin, P. Watkins, R. Andres, and M. Berman. Insulin control of glucose metabolism in man. *J. Clin. Invest.* 55:1057-66, 1975.
64. DeFronzo R.A., J.D. Tobin, and R. Andres. Glucose clamp technique: a method for quantifying insulin secretion and resistance. *Am. J. Physiol.* 237:E214-23, 1979.
65. Simpson R.G., A. Benedetti, G.M. Grodsky, J.H. Karam, and P.H. Forsham. Early phase of insulin release. *Diabetes* 17:684-92, 1968.
66. Reaven G.M., S.W. Shen, A. Silvers, and J.W. Farquhar. Is there a delay in the plasma insulin response of patients with chemical diabetes mellitus? *Diabetes* 20:416-23, 1971.
67. DeFronzo R.A., J.D. Tobin, J.W. Rowe, and R. Andres. Glucose intolerance in uremia: quantification of pancreatic beta cell sensitivity to glucose and tissue sensitivity to insulin. *J. Clin. Invest.* 62:425-35, 1978.

68. Steele R., J. Wall, R. DeBode, and N. Altszuler. Measurement of size and turnover rate of body glucose pool by the isotope dilution method. *Am. J. Physiol.* 187:15-24, 1956.
69. McGuire E.A.H., J.H. Helderman, J.D. Tobin, R. Andres, and M. Berman. Effects of arterial versus venous sampling on analysis of glucose kinetics in man. *J. Appl. Physiol.* 41:565-573, 1976.
70. DeFronzo R., D. Deibert, R. Hendler, P. Felic, and V. Soman. Insulin sensitivity and insulin binding to monocytes in maturity-onset diabetes. *J. Clin. Invest.* 939-46, 1979.
71. Ryan E.A., M.J. Osullivan, and J.S. Skyler. Insulin action during pregnancy: studies with the euglycemic clamp technique. *Diabetes* 34:380-89, 1985.
72. Kruszynska Y.T., G. Petranyi, and K.G.M.M. Alberti. Decreased insulin sensitivity and muscle enzyme activity in elderly subjects. *European J. Clin. Invest.* 18:493-98, 1988.
73. Zuniga-Guajardo S., and B Zinman. The metabolic response to the euglycemic insulin clamp in type I diabetes and normal humans. *Metabolism* 34:926-30, 1985.
74. DeFronzo R.A., R. Hendler, and D. Simonson. Insulin resistance is a prominent feature of insulin-dependent diabetes. *Diabetes* 31:795-801, 1982.
75. Verza M., M. D'Avino, F. Cacciapuoti, E. Aceto, S. D'Errico, M. Varricchio, and D. Giugliano. Hypertension in the elderly is associated with impaired glucose metabolism independently of obesity and glucose intolerance. *J. Hypertens. Suppl.* 6(1):S45-48, 1988.

76. Kruszynska Y., N. Williams, M. Perry, and P. Home. The relationship between insulin sensitivity and skeletal muscle enzyme activities in hepatic cirrhosis. *Hepatology* 8:1615-19, 1988.
77. Marchesini G., G.P. Bianchi, G. Forlani, A.G. Rusticali, D. Patrono, M. Capelli, M. Zoli, P. Vannini, and E. Pisi. Insulin resistance is the main determinant of impaired glucose tolerance in patients with liver cirrhosis. *Dig. Dis. Sci.* 32:1118-24, 1987.
78. Marangou A.G., K.M. Weber, R.C. Boston, P.M. Aitken, J.C. Heggie, R.L. Kirsner, J.D. Best, and F.P. Alford. Metabolic consequences of prolonged hyperinsulinemia in humans. Evidence for induction of insulin insensitivity. *Diabetes* 35:1383-89, 1986.
79. Rizza R.A., L.J. Mandarino, and J.E. Gerich. Mechanism and significance of insulin resistance in non-insulin dependent diabetes mellitus. *Diabetes* 30:990-95, 1981.
80. Burnol A.E., A. Leturque, P. Ferre, and J. Girard. A method for quantifying insulin sensitivity in vivo in the anesthetized rat: the euglycemic insulin clamp technique coupled with isotopic measurement of glucose turnover. *Reprod. Nutr. Develop.* 23(2B):429-35, 1983.
81. Kraegen E.W., D.E. James, S.P. Bennett, and D.J. Chisholm. In vivo insulin sensitivity in the rat determined by euglycemic clamp. *Am. J. Physiol.* 245:E1-7, 1983.
82. Smith D., L. Rossetti, E. Ferrannini, C.M. Johnson, C. Cobelli, G. Toffolo, L.D. Katz, and R.A. DeFronzo. In vivo glucose metabolism in the awake rat: tracer and insulin clamp studies. *Metabolism* 36:1167-74, 1987.

83. Nishimura H., H. Kuzuya, M. Okamoto, K. Yamada, A. Kosaki, T. Kakehi, G. Inoue, S. Kono, and H. Imura. Postreceptor defect in insulin action in streptozotocin-induced diabetic rats. *Am. J. Physiol.* 256:E624-30, 1989.
84. Thorburn A.W., L.H. Storlien, A.B. Jenkins, S. Khouri, and E.W. Kraegen. Fructose-induced in vivo insulin resistance and elevated plasma triglyceride levels in rats. *Am. J. Clin. Nutr.* 49:1155-63, 1989.
85. Storlien L.H., E.W. Kraegen, A.B. Jenkins, and D.J. Chisholm. Effects of sucrose vs starch diets on in vivo insulin action, thermogenesis, and obesity in rats. *Am. J. Clin. Nutr.* 47:420-27, 1988.
86. Kergoat M., D. Bailbe, and B. Portha. Effect of high sucrose diet on insulin secretion and insulin action. A study in rats with non-insulin-dependent diabetes induced by streptozotocin. *Diabetologia* 30:666-73, 1987.
87. Ng S.F., L.H. Storlien, E.W. Kraegen, M.C. Stuart, G.E. Chapman, and L. Lazarus. Effect of biosynthetic human growth hormone on insulin action in individual tissues of the rat in vivo. *Metabolism* 39:264-68, 1990.
88. Hirshman M.F., and E.S. Horton. Glyburide increases insulin sensitivity and responsiveness in peripheral tissues of the rat as determined by the glucose clamp technique. *Endocrinology* 126:2407-12, 1990.
89. Blondel O., J. Simon, B. Chevalier, and B. Portha. Impaired insulin action but normal insulin receptor activity in diabetic rat liver: effect of vanadate. *Am. J. Physiol.* 258:E459-67, 1990.

90. DeFronzo R.A., V. Soman, R.S. Sherwin, R. Hendler, and P. Felig. Insulin binding to monocytes and insulin action in human obesity, starvation, and refeeding. *J. Clin. Invest.* 62:204-13, 1973.
91. Doberne L., M.S. Greenfield, B. Schulz, and G.M. Reaven. Enhanced glucose utilization during prolonged glucose clamp studies. *Diabetes* 30:829-35, 1981.
92. Edelman S.V., M. Laakso, P. Wallace, G. Brechtel, J.M. Olefsky, and A.D. Baron. Kinetics of insulin-mediated and non-insulin-mediated glucose uptake in humans. *Diabetes* 39:955-64, 1990.
93. Laakso M., S.V. Edelman, J.M. Olefsky, G. Brechtel, P. Wallace, and A.D. Baron. Kinetics of in vivo muscle insulin-mediated glucose uptake in human obesity. *Diabetes* 39:965-74, 1990.
94. Finegood D.T., R.N. Bergman, and M. Vranic. Estimation of endogenous glucose production during hyperinsulinemic-euglycemic glucose clamp: comparison of unlabeled and labeled exogenous glucose infusates. *Diabetes* 36:914-24, 1987.
95. Bogardus C., S. Lillioja, D. Mott, G.R. Reaven, A. Kashiwagi, and Foley. Relationship between obesity and maximal insulin-stimulated glucose uptake in vivo and vitro in Pima Indians. *J. Clin. Invest.* 73:800-5, 1984.
96. Lager I., S. Attvall, B.M. Eriksson, H. von Schenk, and U. Smith. Studies on the insulin-antagonistic effect of catecholamines in normal man. Evidence for the importance of B2 receptors. *Diabetologia* 29:409-16, 1986.
97. Nosadini R., S. Del Prato, A. Tiengo, A. Valerio, M. Muggeo, G. Opocher, F. Mantero, E. Duner, C. Marescotti, F. Mollo, and F.

- Belloni. Insulin resistance in Cushing's syndrome. *J. Clin. Endocrinol. Metab.* 57:529-36, 1983.
98. Rizza R.A., L.J. Mandarino, and J.E. Gerich. Cortisol-induced insulin resistance in man: impaired suppression of glucose production and stimulation of glucose utilization due to a postreceptor defect of insulin action. *J. Clin. Endocrinol. Metab.* 54:131-38, 1982.
99. Finegood D.T., R.N. Bergman, and M. Vranic. Modeling error and apparent isotope discrimination confound estimation of endogenous glucose production during euglycemic glucose clamp. *Diabetes* 37:1025-34, 1988.
100. Bell P.M., R.G. Firth, and R.A. Rizza. Assessment of insulin action in insulin-dependent diabetes mellitus using [6-¹⁴C]glucose, [3-³H]glucose, and [2-³H]glucose: differences in the apparent pattern of insulin resistance depending on the isotope used. *J. Clin. Invest.* 78:1479-86, 1986.
101. Argoud G.M., D.S. Schade, and R.P. Eaton. Underestimation of hepatic glucose production by radioactive and stable tracers. *Am. J. Physiol.* 252:E606-15, 1987.
102. Bergman R.N., Y.Z. Ider, C.R. Bowden, and C. Cobelli. Quantitative estimation of insulin sensitivity. *Am. J. Physiol.* 236:E667-77, 1979.
103. Bergman R.N., L.S. Phillips, and C. Cobelli. Physiologic evaluation of factors controlling glucose tolerance in man: measurement of insulin sensitivity and B cell glucose sensitivity from the response to intravenous glucose. *J. Clin. Invest.* 68:1456-67, 1981.

104. Zeleznic A.J., and J. Roth. Demonstration of the insulin receptor in vivo in rabbits and its possible role as a reservoir for the plasma hormone. *J. Clin. Invest.* 61:1363-74, 1978.
105. Bergman R.N., J.C., Beard, and M. Chen. The minimal modeling method: assessment of insulin sensitivity and β -cell function in vivo. In: *Methods in Diabetes Research Vol II: Clinical Methods*. Ed., .L. Clarke, J. Larner, S.L. Pohl, John Wiley & Sons Inc., 1986.
106. Yang Y.J., I.D. Hope, M. Ader, and R.N. Bergman. Insulin transport across capillaries is rate limiting for insulin action in dogs. *J. Clin. Invest.* 84:1620-28, 1989.
107. King G.L., and S.M. Johnson. Receptor-mediated transport of insulin across endothelial cells. *Science (Wash. DC)* 227:1583-83, 1985.
108. King G.L., S.M. Johnson, and I. Jialal. Processing and transport of insulin by vascular endothelial cells: effects of sulfonyureas on insulin receptors. *Am J. Med.* 79:43-47, 1985.
109. Bar R.S., M. Boes, and A. Sandra. Vascular transport of insulin to rat cardiac muscle: central role of the capillary endothelium. *J. Clin. Invest.* 81:1225-33, 1988.
110. Finegood D.T., G. Pacini, and R.N. Bergman. The insulin sensitivity index: correlation in dogs between values determined from the intravenous glucose tolerance test and the euglycemic glucose clamp. *Diabetes* 33:362-68, 1984.
111. Bergman R.N., R. Prager, A. Volund, and J.M. Olefsky. Equivalence of the insulin sensitivity index in man derived by the minimal model method and the euglycemic glucose clamp. *J. Clin. Invest.* 79:790-800, 1987.

112. Donner C.C., E. Frazee, Y.D.I. Chen, C.B. Hollenbeck, J.E. Foley, and G.M. Reaven. Presentation of a new method for specific measurement of in vivo insulin-stimulated glucose disposal in humans: comparison of this approach with the insulin clamp and minimal model techniques. *J. Clin. Endocrinol. Metab.* 60:723-26, 1985.
113. Beard J.C., R.N. Bergman, W.K. Ward, and D. Jr. Porte. The insulin sensitivity index in nondiabetic man: correlation between clamp-derived and IVGTT-derived values. *Diabetes* 35:362-69, 1986.
114. Chen M., R.N. Bergman, G. Pacini, and D.Jr. Porte. Pathogenesis of age-related glucose intolerance in man: insulin resistance and decreased β -cell function. *J. Clin. Endocrinol. Metab.* 60:13-20. 1985.
115. Johnston C., P. Raghu, D.K. McCulloch, J.C. Beard, W.K. Ward, L.J. Klaff, B. McKnight, R.N. Bergman, and J.P. Palmer. β -cell function and insulin sensitivity in nondiabetic HLA-identical siblings of insulin-dependent diabetes. *Diabetes* 36:829-37, 1987.
116. Raghu P., C. Johnston, J.C. Beard, R.N. Bergman, D.K. McCulloch, and J.P. Palmer. Reduced insulin sensitivity in non-diabetic, HLA-identical siblings of insulin-dependent diabetic subjects. *Diabetes* 34:991-94, 1985.
117. Ward W.K., C.L. Johnston, J.C. Beard, T.J. Beneditti, J.B. Jalter, and D. Jr. Porte. Insulin resistance and impaired insulin secretion in subjects with histories of gestational diabetes mellitus. *Diabetes* 34:861-69, 1985.
118. M. Ader, T. Agajanian, D.T. Finegood, and R.N. Bergman. Recombinant deoxyribonucleic acid-derived 22K-human growth hormone generate

- equivalent diabetogenic effects during chronic infusion in dogs. *Endocrinology* 120:725-31, 1987.
119. Yang Y.T., J.H. Youn, and R.N. Bergman. Modified protocols improve insulin sensitivity estimation using the minimal model. *Am. J. Physiol.* 253:E595-602, 1987.
 120. Cutfield W.S., R.N. Bergman, R.K. Menon, and M.A. Sperling. The modified minimal model: application to measurement of insulin sensitivity in children. *J. Clin. Endocrinol. Metab.* 70:1644-50, 1990.
 121. Finegood D.T., I.M. Hramiak, and J. Dupre. A modified protocol for estimation of insulin sensitivity with the minimal model of glucose kinetics in patients with insulin-dependent diabetes. *J. Clin. Endocrinol. Metab.* 70:1538-49, 1990.
 122. Ader M., G. Pacini, Y.J. Yang, and R.N. Bergman. Importance of glucose per se to intravenous glucose tolerance: comparison of the minimal-model prediction with direct measurements. *Diabetes* 34:1092-1103.
 123. Sun J.V., H.M. Tepperman, and J. Tepperman. A comparison of insulin binding by liver plasma membranes of rats fed a high glucose diet or a high fat diet. *J. Lipid Res.* 18:533-39, 1977.
 124. Clement Ip, H.M. Tepperman, P. Holohan, and J. Tepperman. Insulin binding and insulin response of adipocytes from rats adapted to fat feeding. *J. Lipid Res.* 17:588-99, 1976.
 125. Maegawa H, M. Kobayashi, O. Ishibashi, Y. Takata, and Y. Shigeta. Effect of diet change on insulin action: difference between muscles and adipocytes. *Am. J. Physiol.* 251:E616-23, 1986.

126. Zaragoza-Hermans N., and J.P. Felber. Studies of the metabolic effects induced in the rat by a high fat diet. II. Disposal of orally administered (^{14}C)-glucose. *Horm. Metab. Res.* 4:25-30, 1972.
127. Zaragoza N., and J.P. Felber. Studies of the metabolic effects induced in the rat by a high fat diet. I. Carbohydrate metabolism *in vivo*. *Horm. Metab. Res.* 2:323-29, 1970.
128. Collier G.R., K. Chisholm, S. Sykes, P.A. Dryden, and K. O'Dea. More severe impairment of oral than intravenous glucose tolerance in rats after eating a high fat diet. *J. Nutr.* 115:1471-76, 1985.
129. Chisholm K.W., and K. O'Dea. Effect of short-term consumption of a high fat diet on glucose tolerance and insulin sensitivity in the rat. *J. Nutr. Sci. Vitaminol.* 33:377-90, 1987.
130. Lavau M., and C. Susini. [$\text{U-}^{14}\text{C}$]Glucose metabolism *in vivo* in rats rendered obese by a high fat diet. *J. Lipid Res.* 16:134-42, 1975.
131. Susini C., and M. Lavau. *In vitro* and *in vivo* responsiveness of muscle and adipose tissue to insulin in rats rendered obese by a high fat diet. *Diabetes* 27:114-20, 1978.
132. Olefsky J.M., and M. Saekow. The effects of dietary carbohydrate content on insulin binding and glucose metabolism by isolated rat adipocytes. *Endocrinology* 103:2252-63, 1978.
133. Lavau M., S.K. Fried, C. Susini, and P. Freychet. Mechanism of insulin resistance in adipocytes of rats fed by a high-fat diet. *J. Lipid Res.* 20:8-16, 1979.
134. Zaragoza-Hermans N., and J.P. Felber. Studies on the metabolic effects induced in the rat by a high-fat diet. [$\text{U-}^{14}\text{C}$]Glucose metabolism in epididymal adipose tissue. *Eur. J. Biochem.* 25:89-95, 1972.

135. Salans L.B., J.E. Foley, L.J. Wardzala, and S.W. Cushman. Effects of dietary composition on glucose metabolism in rat adipose cells. *Am. J. Physiol.* 240:E175-83. 1981.
136. Watarai T., M. Kobayashi, Y. Takata, I. Sasaoka, M. Iwasaki, and Y. Shigeta. Alteration of insulin-receptor kinase activity by high-fat feeding. *Diabetes* 37:1397-1404.
137. Begum N., H.M. Tepperman, and J. Tepperman. Insulin-induced internalization and replacement of insulin receptors in adipocytes of rats adapted to fat feeding. *Diabetes* 34:1272-77, 1985.
138. Grundleger M.L., and S.W. Thenen. Decreased insulin binding, glucose transport, and glucose metabolism in soleus muscle of rats fed a high fat diet. *Diabetes* 31:232-37, 1982.
139. McGill M.W., and A.N. Rowan. Biological effects of blood loss: implications for sampling volumes and techniques. 31:5-18, 1989.
140. Bergman R.N., C. Cobelli, and G. Toffolo. Minimal models of glucose/insulin dynamics in the intact organism. A novel approach for evaluation of factors controlling glucose tolerance. *Trans. Inst. M C* 3:207-16, 1981.
141. McIntosh J.E.A., and R.P. McIntosh. Modelling in biology. Mathematical descriptions of biological models. In: *Mathematical modelling and computers in endocrinology*. Ed., McIntosh J.E.A., and R.P. McIntosh., Springer-Verlag, pp1-73, 1980.
142. Williams R.H. Somatostatin. In: *Textbook of endocrinology*. Sixth edition. Ed., Williams R.H., pp702-39, 1981.
143. Longo C.J., B.W. Tobin, I.M. Hramiak, J. Dupre, and D.T. Finegood. A somatostatin modified glucose tolerance test for estimation of insulin sensitivity using the minimal model in the rat. In press.

144. Wu M.S., L.T. Ho, J.J. Chen, Y.D.I. Chen, and G.M. Reaven.
Somatostatin potentiation of insulin-induced glucose uptake in normal individuals. *Am. J. Physiol.* 251:E674-79, 1986.
145. Bergman R.N., M. Ader, D.T. Finegood, and G. Pacini.
Extrapancreatic effect of somatostatin infusion to increase glucose clearance. *Am. J. Physiol.* 247:E370-79, 1984.
146. Baron A.D., P. Wallace, G. Brechtel, and R. Prager. Somatostatin does not increase insulin-stimulated glucose uptake in humans. *Diabetes* 36:33-36, 1987.
147. Stevenson R., K.E. Steiner, P.E. Williams, and A.D. Cherrington.
Lack of effect of somatostatin on epinephrine-stimulated glucose production in the dog. *Metabolism* 36:451-57, 1987.
148. Meneilly G.S., D. Elahi, K.L. Minaker, and J.W. Rowe. Somatostatin does not alter insulin-mediated glucose disposal. *J. Clin. Endocrinol. Metab.* 65:364-67, 1987.
149. Shangraw R.E., F. Jahoor, H. Miyoshi, W.A. Neff, C.A. Stuart, D.N. Herndon, and R.R. Wolfe. Differentiation between septic and postburn insulin resistance. *Metabolism* 38:983-89, 1989.
150. Yki-Jarvinen H., K. Sammalkorpi, V.A. Koivisto, and E.A. Nikkila.
Severity, duration, and mechanisms of insulin resistance during acute infections. *J. Clin. Endocrinol. Metab.* 69:317-23, 1989.
151. Lang C.H., C. Dobrescu, and K. Meszaros. Insulin-mediated glucose uptake by individual tissues during sepsis. *Metabolism* 39:1096-1107, 1990.
152. Lang C.H., and C. Dobrescu. Gram-negative infection increases noninsulin-mediated glucose disposal. *Endocrinology* 128:645-53, 1991.

153. Lang C.H., C. Dobrescu, G.J. Bagby, and J.J. Spitzer. Altered glucose kinetics in diabetic rats during Gram-negative infection. *Am. J. Physiol.* 253:E123-29, 1987.
154. Lang C.H., and C. Dobrescu. Sepsis-induced changes in *in vivo* insulin action in diabetic rats. *Am. J. Physiol.* 257:E301-8, 1989.